USING A TISSUE-ENGINEERED VASCULAR MODEL TO DEVELOP MAST CELLS FROM STEM CELLS

By

TSZWAI REGINA CHAN

Bachelor of Science in Chemical Engineering

Arizona State University

Tempe, Arizona

2011

Submitted to the Faculty of the
Graduate College of the
Oklahoma State University
in partial fulfillment of
the requirements for
the Degree of
MASTER OF SCIENCE
July, 2018

USING A TISSUE-ENGINEERED VASCULAR

MODEL TO DEVELOP MAST CELLS

FROM STEM CELLS

Thesis Approved:

Dr. Heather Gappa-Fahlenkamp

Thesis Adviser

Dr. Joshua D. Ramsey

Dr. James H. Meinkoth

To Fermium and Nikola.

ACKNOWLEDGMENTS

This thesis would not have been possible without the dedication, guidance, and support of professors, colleagues, family members and friends. I would especially like to thank my graduate committee for their mentorship and professional training. I was privileged to have Dr. Fahlenkamp as an advisor and mentor. Dr. Fahlenkamp gave me the opportunity to conduct research in one of the most exciting fields of today. She was patient in training me to become a professional. Dr. Ramsey offered consistent support and encouragement. To Dr. Meinkoth, I would like to thank you for the tireless mentoring, guidance and motivation throughout my research. He offered countless pieces of advice and suggestions on many aspects of this research.

To my family, thank you for encouraging me in all of my pursuits. Sincere thanks goes to Frankie for his unconditional support, encouragement, and the hundreds of videos of Tohfee. Lastly, I would especially like to thank Ryan Hugg, I would not make it without you.

Thank you all.

Name: TSZWAI REGINA CHAN

Date of Degree: JULY, 2018

Title of Study: USING A TISSUE-ENGINEERED VASCULAR MODEL TO DEVELOP MAST CELLS FROM STEM CELLS

Major Field: CHEMICAL ENGINEERING

Abstract: Over the last few decades, the prevalence of allergic diseases has increased dramatically in developed nations. Mast cells (MCs) play a key role in allergic responses. However, it is difficult to isolate high numbers of viable and mature MCs. Others have determined methods to grow MCs in traditional two-dimensional (2D) cell culture from various adult stem cell sources. Our previous studies have shown that it is possible to develop committed MC precursors in a 3D extracellular matrix-like environment. Our long-term goal is to develop a tissue-engineered vascular model that includes $CD133^+$ hematopoietic stem cells (HSCs) along with fibroblasts within a 3D matrix, to represent the tissue space, and a layer of endothelial cells (ECs) on one surface, to represent the capillary endothelium. The objectives of this project were to identify which source of adult human $CD133^+$ HSCs generated the greatest number of viable and mature MCs within the model and to determine the effect of fibroblasts and ECs to the growth and differentiation of MCs within the model. HSCs from human adult peripheral blood mononuclear cells (PBMC), adult granulocyte colony-stimulating factor-mobilized peripheral blood mononuclear cells (G-PBMC), and cord blood were mixed with fibroblasts within a collagen matrix and incubated with StemSpan media supplemented with cytokines. Samples were incubated for eight weeks, with ECs seeded on the surface of the matrix in the last week. MCs were characterized based on cell morphology, viability, intracellular stores of preformed factors, cell surface marker expression, and the release of soluble mediators. The results show that HSCs isolated from G-PBMC generated the greatest number of viable and mature MCs within the 3D co-culture model. The data demonstrated that 3D co-culture system had a higher yield of mature MCs than the traditional 2D cell culture system without fibroblasts and ECs.

TABLE OF CONTENTS

Chapter **Page**

Chapter **Page**

LIST OF FIGURES

Figure **Page**

CHAPTER I

INTRODUCTION

Over the last few decades, the prevalence of allergic diseases has increased dramatically in developed nations. Allergic disease is the 5th leading chronic disease in the United States among all ages, and the 3rd most common chronic disease among children under 18 years old [1]. A recent nationwide survey found that more than half of all U.S. citizens test positive to one or more allergens [2]. The cost associated with allergic diseases are more than 7 billion dollars per year [1]. Basic and clinical studies suggest that inflammation plays a role not only in obvious allergic responses, such as in asthma and eczema, but also ailments just recently associated with inflammation—such as atherosclerosis, Alzheimer's disease, colon cancer, and diabetes. Therefore, the study of inflammation not only contributes to the study of allergic diseases, but also has much wider implications associated with the possible involvement of inflammation in the underlying mechanisms of other types of diseases, leading to possible clues to the prevention or treatment of these other diseases.

Few tools are available currently to study allergic reactions and inflammation. Animal studies, clinical studies, and monolayers of cultured cells (2D cell culture) have contributed to our current understanding of allergy and have provided valuable

information toward our understanding of inflammatory mediators, cellular and tissue specific responses, and medical interventions. The inherent limitation of animal models is that they do not generally translate to human responses, especially in the case of allergic responses [3-7]. The usefulness of human tests is limited by their empirical nature, dependence on trial and error approaches, and the possibility of severe complications [8-12]. Cell culture of various animal and human cells has been used to study allergic reactions *in vitro* [13, 14]. However, a 2D cell culture system cannot completely recapitulate the organized cellular structure of tissues *in vivo*. To approximate the *in vivo* microenvironment within an *in vitro* system, 3D models are more appropriate. The 3D tissue environment affects integrin ligation, cell contraction, and associated intracellular signaling [15, 16]. A 3D matrix is also important for solute diffusion and interaction with growth factors and enzymes resulting in tissue-scale solute concentration gradients and intercellular gradients. Furthermore, a 3D environment is necessary to model morphogenetic and remodeling events that occur over larger-length scales, such as epithelial acinar formation [17, 18] and cluster formation in studies of T lymphocyte-cell behavior [19]. Our long-term goal is to develop 3D tissue-engineered skin and mucosal models that contains multiple human cell types within a 3D environment that provides for cell movement and interaction, in order to investigate some of the key aspects of an allergic inflammatory response. In addition, to recapitulate an *in vivo* inflammatory response, the 3D tissue-engineered systems must contain the relevant cell types.

Mast cells (MCs) are considered the central effector cells in the early events associated with allergic inflammatory responses [20-23]. Poised at the interface of the external environment in the skin and at mucosal surfaces, MCs are among the first cells to

encounter antigens that elicit allergic reactions [24]. The high-affinity immunoglobulin E (IgE) receptor on MCs, FcεRI, associates with IgE through its Fc region and forms a stable antigen receptor [15, 16, 25]. Upon binding multivalent allergen via this antigen receptor, MCs are activated and immediately release preformed mediator, such as histamine and neutral proteases like tryptase and chymase, present in their granules,. Activated MCs also synthesize and release other inflammatory mediators, such as prostaglandin D2 (PGD2), monocyte chemoattractant protein-1 (MCP-1), macrophage inflammatory protein-1 (MIP-1), tumor necrosis factor-alpha (TNF-α), granulocyte-macrophage colony-stimulating factor (GM-CSF), interleukin-8 (IL-8), and IL-4 [26-31]. Changes in the expression of adhesion molecules and costimulatory or inhibitory molecules occur with MC activation. Collectively, these mediators initiate rapid vascular permeability and leukocyte recruitment [32-34].

Few studies have investigated normal, human MCs in culture. There are considerable difficulties in isolating and analyzing MC populations directly *ex vivo*. Unlike lymphocytes and monocytes, MCs do not circulate, but remain relatively fixed and dispersed in tissues under basal conditions. Thus, there is no good repository of fully mature MCs from which to draw, in order to study their function *ex vivo*. The secondary lymphoid organs normally contain resident MCs; however, even in inflammatory settings in which additional MCs migrate to the lymph nodes, the relative scarcity of cells, when compared with T cells or B cells, for example, prevents their use in any functional assays. Most early studies of MCs relied on the use of transformed MCs [35-38]. Although such cells have been instrumental in delineating MC signaling pathways and in revealing the wide variety of cytokines and chemokines that MC express, they are not useful for

assessing *in vivo* function. The ability of MC differentiation factors, such as interleukin-3 (IL-3) and stem cell factor (SCF), to act on CD133+/CD34+ progenitor cells isolated from peripheral blood, bone marrow, cord blood, or fetal liver have made it possible to grow large numbers of committed MC precursors [39-44]. These cells express high levels of the high-affinity IgE receptor FcεRI, contain preformed mediators that are present in MC granules, and express some of the inducible MC mediators associated with more mature tissue MCs [43].

The traditional 2D culture methods most commonly use a single cell type and grow cells on a culture dish or flask. Many studies rely on the 2D method to generate MCs using peripheral blood, cord blood or bone marrow-derived progenitor cells. For this study, the most common cell sources such as peripheral blood and cord blood were selected to generate MCs within a tissue-engineered vascular model [45-48]. The 2D cell culture method that was used in this study was selected based on previous studies [46, 49-51].

In order to create tissue-engineered models to study an allergic inflammatory response, we would need to be able to generate MCs from progenitor cells within the models, since it is difficult to obtain primary cells. In a previous study, we have shown for the first time that it is possible to develop committed MC precursors in a 3D extracellular matrix-like environment and that these cells are different than those generated from 2D cell culture systems [52]. For this project, we have developed a 3D tissue-engineered vascular model that includes $CD133^{+}$ hematopoietic stem cells along with fibroblasts within a 3D matrix, to represent the tissue space, and a layer of endothelial cells (ECs) on one surface, to represent the blood endothelium. Studies have shown that tissue fibroblasts and ECs contribute to the growth and differentiation of MCs, but the exact mechanisms are not

fully known [53, 54]. **We hypothesize that the tissue-engineered vascular model can be used to develop MCs from stem cell sources and that the cells are more functional than those developed in 2D cell culture systems due to the influence of fibroblasts and ECs.** To test our hypothesis as an initial step towards our long-term goal, it is necessary to complete the following project objectives:

Objective 1: Identify which source of human $CD133^+$ hematopoietic stem cells generates the greatest number of viable and mature MCs within a 3D tissue-engineered vascular model. Based on the use of various cell sources in previous studies, we hypothesize that one source will result in the greatest number of viable and mature MCs within the 3D culture system.

Objective 2: Determine the effect of fibroblasts and ECs on the growth and differentiation of MCs within the 3D tissue-engineered vascular model. Unlike previous cell culture systems, the 3D culture system allows cells to interact with each other through direct contact and by soluble factors. We will take advantage of this unique property to investigate the generation of MCs within the 3D tissue-engineered model compared to those in the 2D culture system.

By meeting the project objectives, the following significant outcomes are possible: 1) the development of an advanced tissue culture system that can generate large numbers of viable and mature MCs to be used by researchers to study allergic responses, as well as the role of inflammation associated with many disease states; 2) new information about how stem cells develop within a 3D microenvironment; and 3) a better understanding of the role of fibroblasts and ECs in MC development and maintenance.

CHAPTER II

MATERIALS AND METHODS

2.1. Antibodies and reagents

StemSpan™ Serum-Free Expansion Medium (SFEM) cell culture medium was purchased from STEMCELL Technologies (Vancouver, Canada). Human stem cell factor (SCF), interleukin (IL)-3, and IL-6 were obtained from PeproTech (Rocky Hill, NJ). Defined HyClone fetal bovine serum (FBS) was from GE Healthcare Life Sciences (Logan, UT). Zombie Green™ fixable viability kit, anti-human fluorochrome-conjugated CD117/c-kit (clone 104D2), FcεRI (clone CRA-1), CD31 (clone WM59), and the isotype controls, mouse IgG1 (clone MOPC-21), mouse IgG2b (clone MPC-11) were obtained from BioLegend (San Diego, CA). Human myeloma IgE was from Athens Research & Technology (Athens, GA). Goat anti-human IgE was acquired from Chemicon International (Temecula, CA).

2.2. Isolation of human $CD133^+$ cells

2.2.1. Adult peripheral blood mononuclear cells (PBMCs)

PBMCs were isolated from fresh leukocyte preparations (obtained from the Oklahoma Blood Institute; Oklahoma City, OK) by the Ficoll-Paque density separation method (GE

Healthcare). $CD133^+$ cells were isolated from PBMCs using a magnetic separation kit (MACS Miltenyi Biotec; Auburn, CA), following the manufacturer's protocol.

2.2.2. Cord blood (CB)

$CD133^+$ cells from human cord blood were purchased from PromoCell (Heidelberg, Germany). Hematopoietic progenitor expansion medium DXF and cytokine mix E, also from PromoCell, were used to expand the cells, following the manufacturer's protocol.

2.2.3. Granulocyte-colony-stimulating factor (G-CSF)-mobilized PBMCs

$CD133^+$ cells were obtained from G-CSF-mobilized PBMCs (obtained from Blood and Marrow Transplantation Program; University of Oklahoma, Oklahoma City, OK) by magnetic separation, as described previously.

2.3. $CD133^+$ Cell Culture

$CD133^+$ cells were cultured following a previously described protocol (Andersen, 2008). Briefly, the cells (50,000 cells/ml) were seeded in StemSpan medium supplemented with SCF (100 ng/ml), IL-6 (50 ng/ml), and IL-3 (1 ng/ml) (hitherto referred to as "supplemented media") for the first three weeks with weekly media changes. After three weeks, IL-3 was removed from the media. One week prior to analysis, FBS (10%, v/v) was added to the media. Samples were monitored weekly by contrast microscopy.

2.4. Endothelial cell (EC) Culture

Human umbilical vein endothelial cells (ECs) purchased from PromoCell were seeded in flasks coated with fibronectin (25 μg/mL; Alfa Aesar, Tewksbury, MA). ECs were cultured in EC Growth Medium MV with supplement Mix (PromoCell) with media

changes every 72 h, until ECs reached >70% confluency. The medium was replaced with StemSpan medium supplemented with 20% FBS for 24 h prior to use in the 3D tissue-engineered vascular model.

2.5. 3D tissue-engineered vascular model with fibroblasts and ECs

Frozen FibroGRO^{TM} xeno-free mitomycin C treated human foreskin fibroblasts purchased from Millipore Sigma (Burlington, MA) were thawed and added to serum-free StemSpan medium, until ready for use. A 2 mg/ml collagen solution was prepared, as described by Derakhshan et al., using 64.5 vol% of 3.1 mg/ml type 1 bovine collagen (Advanced BioMatrix, Carlsbad, CA), 8.1 vol% 10× M199, 13.3 vol% 0.1N NaOH, and 14.1 vol% PBS. The collagen solution was mixed with CD133^{+} progenitor cells (6.8 $\times 10^4$ cells/ml) and fibroblasts (4.0 $\times 10^4$ cells/ml) and added to 48-well cell culture plates. After 45 mins, the collagen-cell solution formed a gel and supplemented media was added to the samples, with media changes once a week. After three weeks, IL-3 was removed from the media. One week prior to analysis, samples were coated with a fibronectin solution (25 μg/mL) and seeded with ECs (5.5 $\times 10^4$ cells/cm^2) in the StemSpan medium supplemented with 20% FBS.

2.6. Characterization of CD133^{+}-derived MCs

2.6.1 Yield and granule formation

The number of viable MCs and MC granule formation was studied using Wright-Giemsa to stain metachromatic cells [45]. To collect cells from the 3D tissue-engineered vascular model, the collagen matrix was digested by incubation with 2 mg/ml of collagenase D

(Roche Applied Science; Indianapolis, IN) for 1 h. The collected cells were counted using a hemocytometer and the number of viable cells was determined by Trypan blue exclusion method. Cytosolic granule formation was determined by Wright-Giemsa staining using an automated stainer (Ames Hema-Tek Stainer). MC ratio was calculated as the ratio of the granular cells to the non-granular cells. Cell yield was calculated as the ratio of the number of viable, granular cells harvested from the system to the number of cells seeded.

2.6.2 Phenotypic marker expression

Expression of c-kit and FcεRI was assessed by flow cytometry. After the culture period, the expression of FcεRI was stabilized by incubating the cells for 24 h with myeloma IgE (2 μg/ml). Cells were collected and stained using anti-c-kit, anti-FcεRI, or relevant isotype controls, and analyzed by flow cytometry. Viable cells were determined by staining with the Zombie Green™ fixable viability kit.

For immunocytochemical staining of tryptase and chymase granules, cells were collected and fixed using a fixation/permeabilization solution kit (BD Biosciences; CA). After incubation with a blocking solution containing 10% goat serum (v/v%, Gibco; CA) for 1 h, cells were incubated with primary antibodies against tryptase, chymase, or relevant isotype controls. Next, a secondary antibody was added and incubated for 30 min at room temperature. The cells were incubated for at least 1 h in the staining buffer containing 0.2% bovine serum albumin (BSA), prior to staining with anti-c-kit antibody and analysis by flow cytometry.

2.6.3 $CD133^{+}$-derived MC activation

After the culture period, function of the generated MCs was examined by cross-linking the FcεRI receptors by IgE and anti-IgE antibodies for cell activation [45]. Cells were sensitized with 15 μg/ml myeloma IgE (Athens Research & Technology; Athens, GA) in complete media for 24 h and rinsed three times prior to activation with 25 μg/mL of anti-IgE (Chemicon International Inc.; Temecula, CA) in Tyrode's solution (Boston BioProducts; Ashland, MA) supplemented with SCF and IL-6 for 1 h. For the 3D tissue-engineered vascular model, cells were activated within the collagen matrix.

2.6.4 Gene expression

For gene expression in response to activation, cells were collected and total RNA was extracted using TRI Reagent (Molecular Research Center, Cincinnati, OH) following manufacturer's protocol. UltraPure™ Glycogen (0.5 mL; ThermoFisher Scientific) was included as a carrier for nucleic acid precipitation in ethanol. After DNase I treatment, 1 mg of total RNA was used to synthesize complementary DNA (cDNA) using a cDNA synthesis kit (Thermo Fisher Scientific). Real-time PCR was performed using an ABI 7500 fast Real-time PCR System (Applied Biosystems, Foster City, CA) and a reaction mixture qPCR MasterMix Plus (SYBR Green 2 · PCR Master Mix, a cDNA template, and forward and reverse primers). Primer sequences were as follows: (beta-actin-FW: GCCGGGACCTGACTGACTAC; beta-actin-RE: TTCTCCTTAATGTCACGCACGAT; PGD2-FW: GGCGTTGTCCATGTGCAAG; PGD2-RE: GGACTCCGGTAGCTGTAGGA; MCP-1 (CCL2)-FW: CAGCCAGATGCAATCAATGCC; MCP-1 (CCL2)-RE:

TGGAATCCTGAACCCACTTCT; IL-8-FW: ACTGAGAGTGATTGAGAGTGGAC; IL-8-RE: AACCCTCTGCACCCAGTTTTC; MIP-1α-FW: AGTTCTCTGCATCACTTGCTG; MIP-1α-RE: CGGCTTCGCTTGGTTAGGAA; TNF-α-FW: CCTGCTGCACTTTGGAGTGAT; TNF-α-RE: CAACATGGGCTACAGGCTTGT; IL-4-FW: GCAGCTGATCCGATTCCTGA; IL-4-RE: TCCAACGTACTCTGGTTGGC; GM-CSF-FW: TCCTGAACCTGAGTAGAGACAC; GM-CSF-RE: TGCTGCTTGTAGTGGCTGG). Primers were synthesized by Sigma-Aldrich. Relative expression levels of PGD2, MCP-1, IL-8, MIP-1α, TNF-α, IL-4, and GM-CSF were normalized to that of b-actin (housekeeping gene) expression using the 2-DDCT method [55].

2.6.5 Histamine content and release

For measuring histamine release, culture media without cells was collected. For measuring the histamine content in the generated MCs, cells were collected and lysed by freeze-thaw cycles in water and sonication for 5 min [56]. Histamine was quantified using a histamine-specific ELISA (RefLab ApS; Copenhagen, Denmark) following the manufacturer's protocol. The percentage of total histamine release was determined by the amount of histamine released by the cells in the culture media compared to the total histamine content, which included the extracellular histamine release and the intracellular histamine content.

2.7 Statistical analysis

Experimental results are expressed as the mean ± standard deviation of triplicate samples. For testing multiple groups, analysis of variance was used to determine whether there is a

significant difference between any of the groups (p-value < 0.05). Differences between two groups were determined using Student's t-test, with a p-value < 0.5 considered significant. Statistical analyses were done using GraphPad Prism (GraphPad Software, San Diego, CA). Microscopic images shown are representative of analyzed samples.

CHAPTER III

RESULTS

3.1. Identifying which source of adult human CD133+ hematopoietic stem cells generates the greatest number of viable and mature MCs within a 3D tissue-engineered vascular model.

3.1.1. Cell density

Cell density increased for peripheral blood (PB)-, cord blood (CB)- and granulocyte colony-stimulating factor-mobilized peripheral blood mononuclear cell (G-PBMC)-derived cells after eight weeks of culture in the 3D tissue-engineered vascular model, as shown in Fig. 1. The microscopy images showed the cell concentrations increasing with the time in culture. For each time point examined, there was no significant difference in cell density among the samples.

3.1.2. Morphology

Cell morphology was examined at Weeks 2, 4 and 8 by metachromatic staining using Wright-Giemsa and examined by contrast microscopy (Fig. 2).

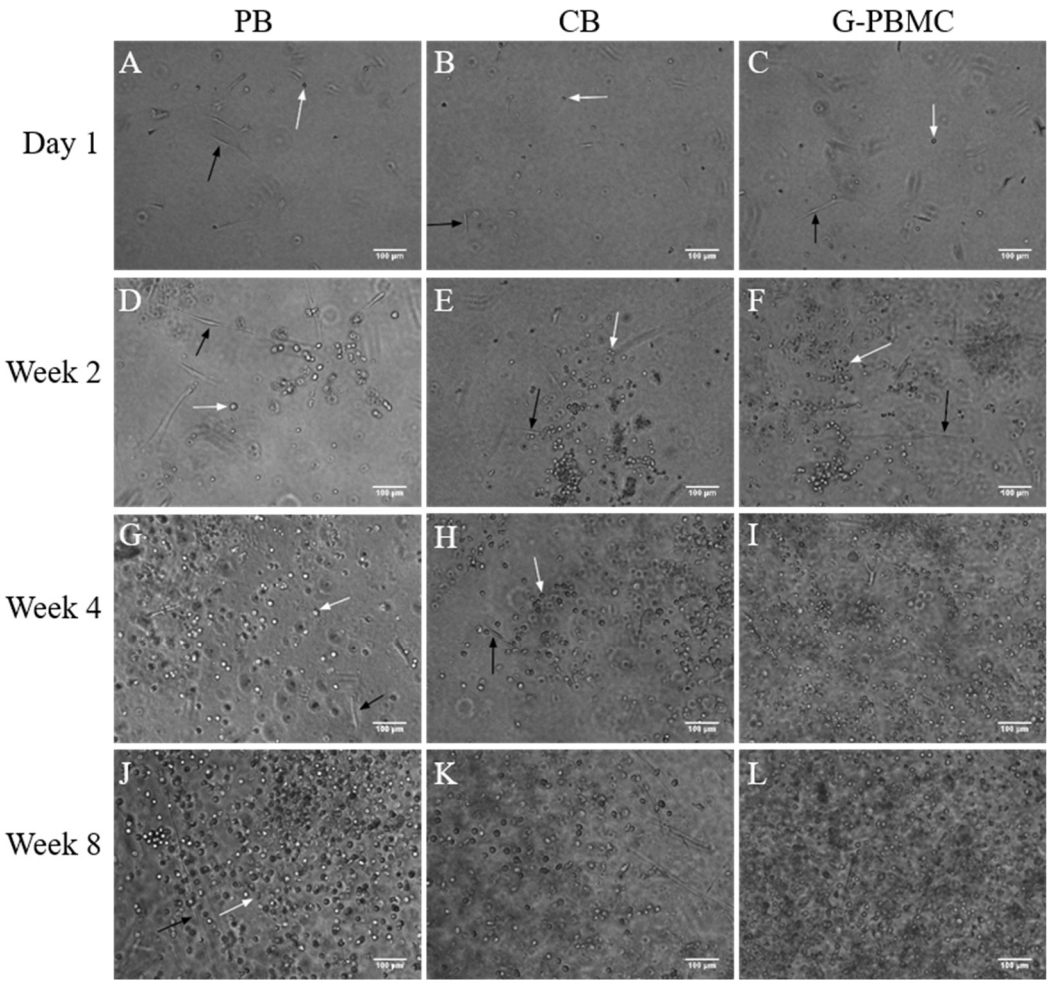

Figure 1. Increasing cell density for peripheral blood (PB)-, cord blood (CB)- and granulocyte colony-stimulating factor-mobilized peripheral blood mononuclear cells (G-PBMC)-derived cells over eight weeks in a 3D tissue-engineered vascular model with fibroblasts and endothelial cells. Samples were examined by phase contrast microscopy once a week. Representative images are shown for triplicate samples of each group. White arrows point to typical mast cells (MCs). Black arrows point to typical fibroblasts. J-L) Endothelial cells were added to the cells at Week 8.

The average size of the cells generated from $CD133^+$ hematopoietic stem cells (HSCs) from PB was estimated to be 46.07 ± 9.96 μm, CB was estimated to be 35.17 ± 7.98 μm and G-PBMC was estimated to be 21.49 ± 3.34 μm after eight weeks of culture. The cells generated from $CD133^+$ HSCs from three different sources grown in the 3D tissue-engineered vascular model with fibroblasts and ECs showed signs of maturity with secretory granules stained blue or violet (Fig.2).

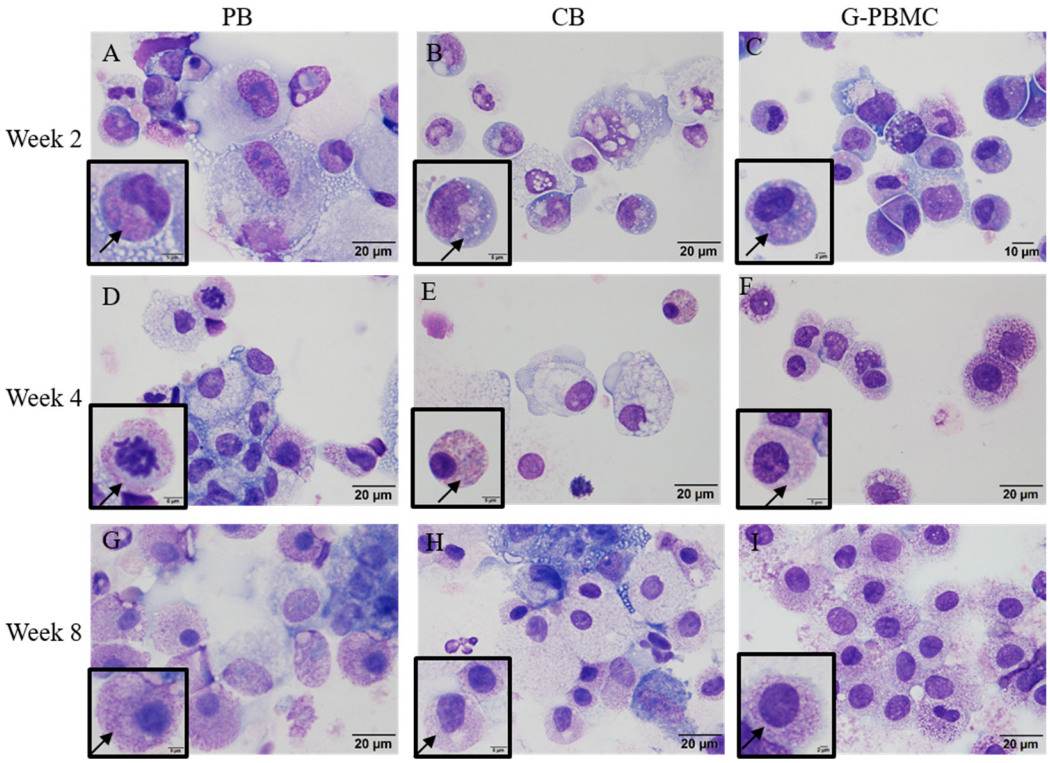

Figure 2. Morphological changes of peripheral blood (PB)-, cord blood (CB)- and granulocyte colony-stimulating factor-mobilized peripheral blood mononuclear cells (G-PBMC)-derived cells over eight weeks in a 3D tissue-engineered vascular model with fibroblasts and endothelial cells. Cells were stained with Wright-Giemsa and examined by light microscopy. Representative images are shown for triplicate samples of each group. The granules of mast cells (MCs) stain a deep blue to violet. Data are represented as mean ±SD; n=3. * indicates $p < 0.05$.

3.1.3. Proliferation / Relative cell yield

The cells generated from G-PBMC-derived $CD133^+$ HSCs showed a high number of granular cells and significantly greater cell yield compared with other cell sources. Cells generated from CB-derived $CD133^+$ HSCs had the lowest number of granular cells and relative cell yield compared with the other two cell sources.

3.1.4. Expression of FcεRI in c-kit^+ population

The cells generated from PB-derived $CD133^+$ HSCs that showed c-kit^+/$Fc\varepsilon RI^+$ expression increased from 19.06 ± 0.05% to 98.19 ± 1.43% after eight weeks of culture. The cells

generated from CB-derived CD133$^+$ HSCs that showed c-kit$^+$/FcεRI$^+$ expression decreased from 71.02 ± 1.37% to 12.45 ± 0.23%. G-PBMC-derived progenitor cells with c-kit$^+$/FcεRI$^+$ expression increased from 18.64 ± 1.41% to 91.97 ± 0.34% after eight weeks of culture in the 3D tissue-engineered vascular model. Cells were analyzed using

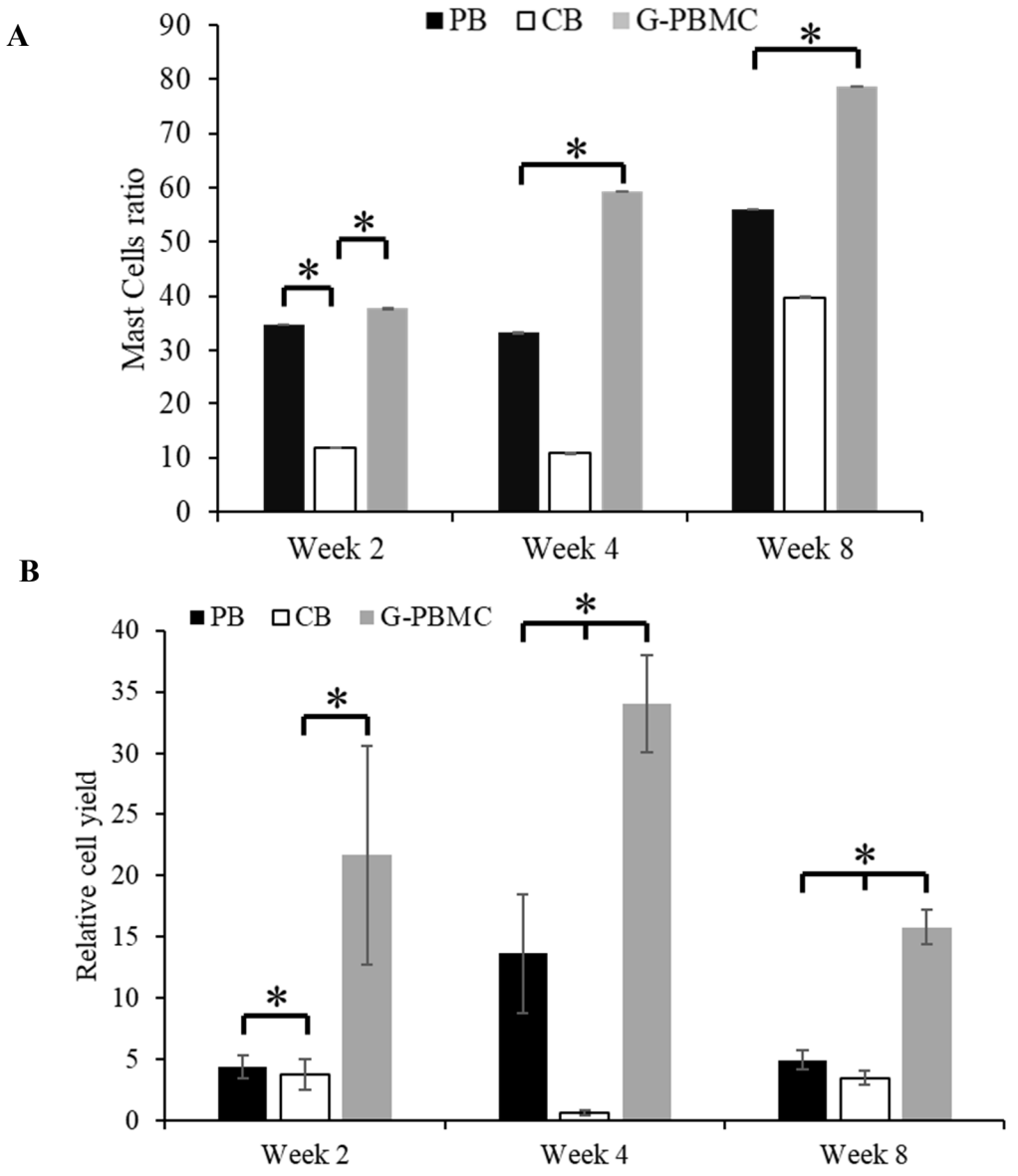

Figure 3. A) Ratio of granular mast cells (MCs) compared with non-granular cells for peripheral blood (PB)-, cord blood (CB)- and granulocyte colony-stimulating factor-mobilized peripheral blood mononuclear cells (G-PBMC)-derived cells in a 3D tissue-engineered vascular model with fibroblasts and endothelial cells. B) Relative cell yield for the number of granular MCs compared to the number of initial CD133$^+$ cells from all three cell sources that were seeded in the 3D tissue-engineered vascular tissue model. Data are represented as mean ± SD; n=3. * indicates $p < 0.05$.

flow cytometry after two, four and eight weeks. The gating strategy and representative density plots are shown in Fig. 4A. The cells were first gated based on their viability.

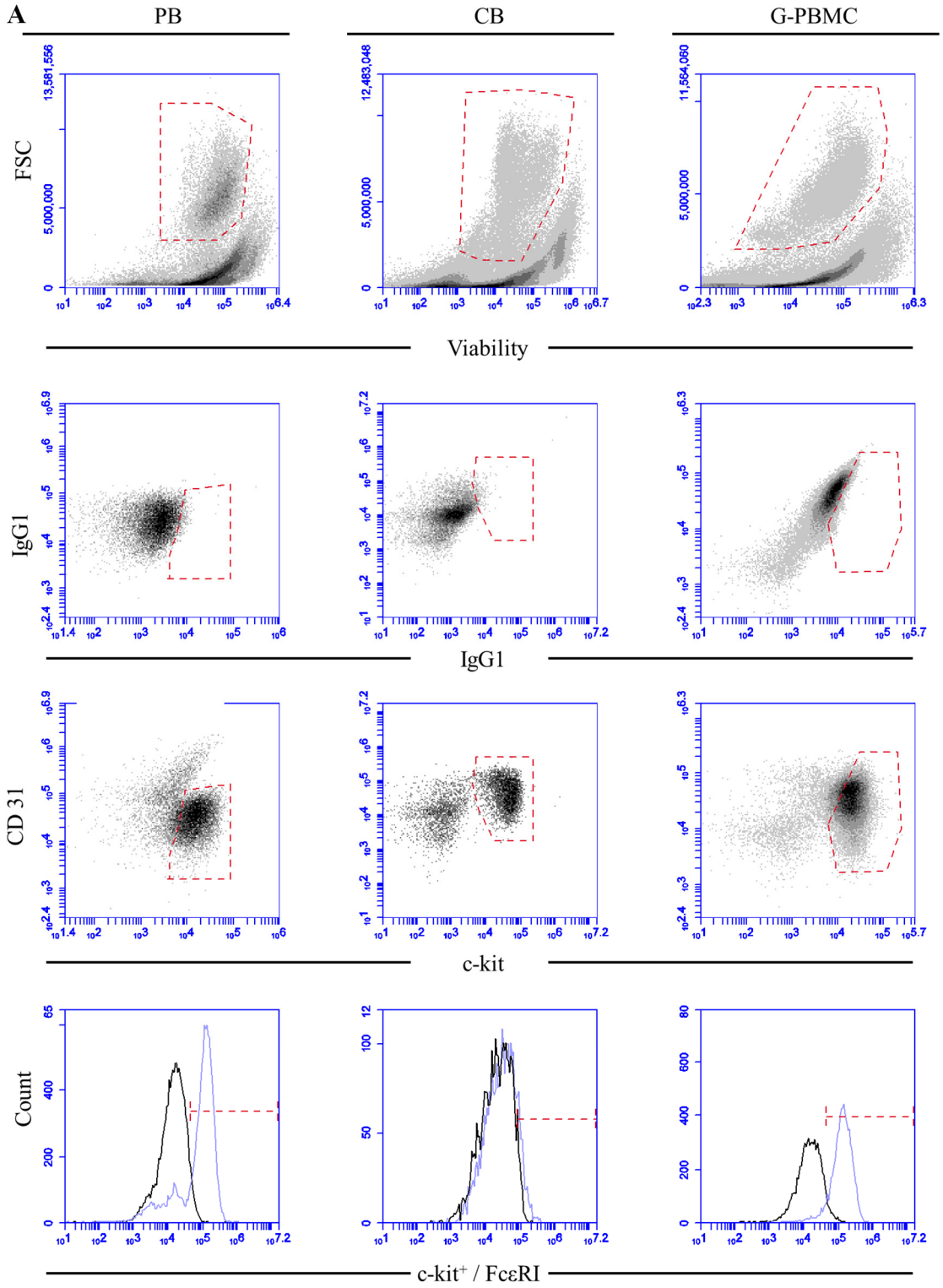

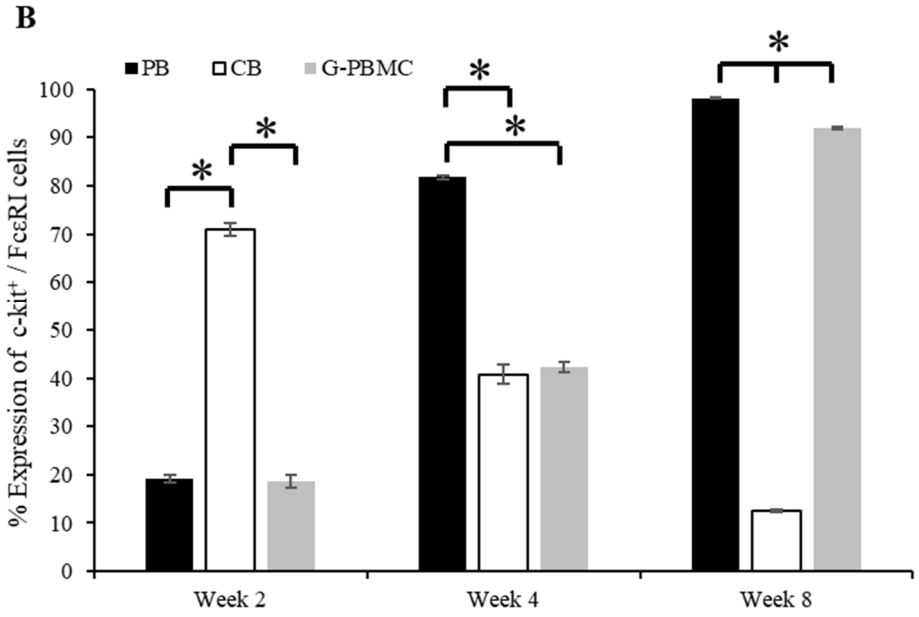

Figure 4. Expression of c-kit$^+$/FcεRI$^+$ cells derived from peripheral blood (PB)-, cord blood (CB)- and granulocyte colony-stimulating factor-mobilized peripheral blood mononuclear cells (G-PBMC)-derived CD133$^+$ progenitor cells during eight weeks of culture in a 3D tissue-engineered vascular model with fibroblasts and endothelial cells. A) The gating scheme and representative density plots of the expression of phenotypic markers. B) Percentage of c-kit$^+$/FcεRI$^+$ cells. Data are represented as mean ± SD; n=3. * indicates $p < 0.05$.

Next, the c-kit$^+$ population was gated and compared with isotype. The expression of FcεRI in the c-kit$^+$ population was then measured using histograms (Fig. 4B).

3.1.5. Expression of tryptase and chymase

The expression of tryptase and chymase by MCs derived from all three sources was measured by flow cytometry after two, four and eight weeks (Fig. 5A). The gating strategy is shown in Fig. 5A. MCs were selected based on the cell size and granularity as forward scatter (FSC) and side scatter (SSC) parameters. The MCs generated from CD133$^+$ HSCs derived from all three sources displayed high levels of tryptase expression (>80%) after eight weeks of culture in the 3D culture system (Fig. 5B). As shown in Fig.

5C, >60% MCs generated from PB-and G-PBMC-derived CD133^{+} HSCs expressed chymase.

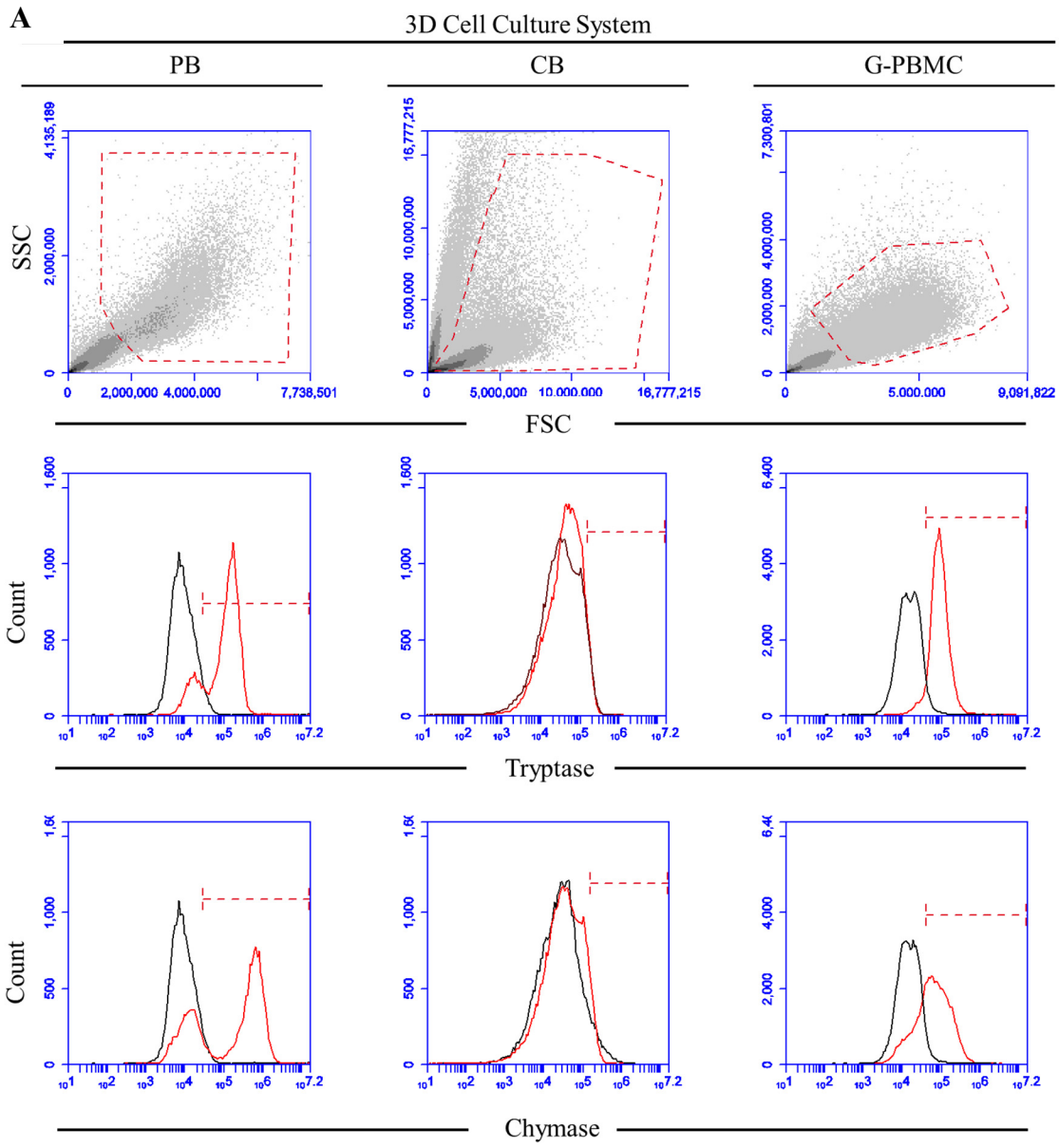

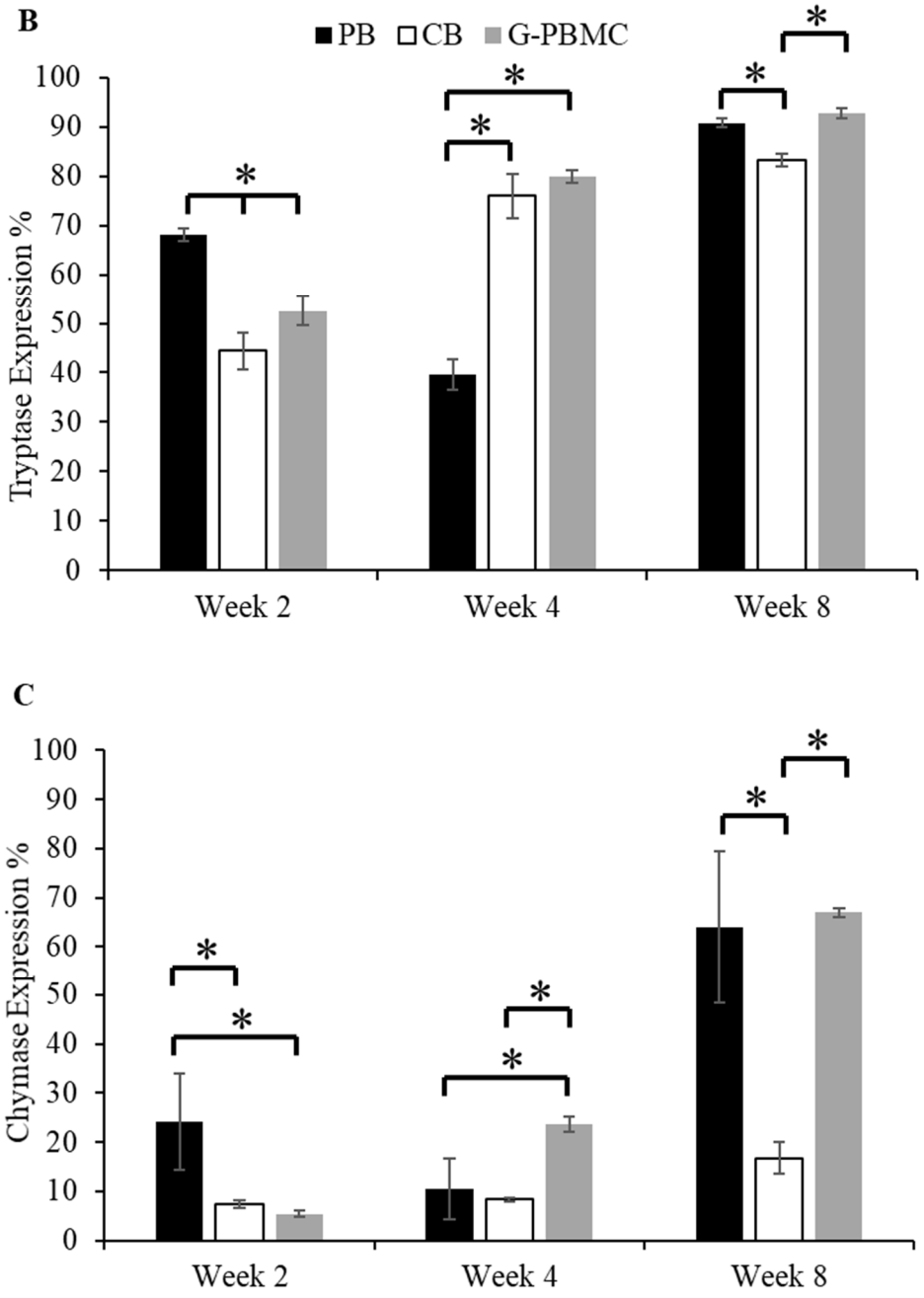

Figure 5. Expression of tryptase and chymase in cells differentiated from peripheral blood (PB)-, cord blood (CB)- and granulocyte colony-stimulating factor-mobilized peripheral blood mononuclear cells (G-PBMC)-derived $CD133^{+}$ progenitor cells after eight weeks in a 3D tissue-engineered vascular model with fibroblast and endothelial cells. A) The gating strategy to identify tryptase and chymase population; percentage of B) tryptase and C) chymase expression. Data are represented as mean ± SD; n=3. * indicates $p < 0.05$.

3.1.6. Histamine content and histamine release

The release of histamine was examined to determine the functionality of MCs. In the 3D culture system, MCs generated from G-PBMC-derived $CD133^+$ HSCs showed the highest histamine content compared with cells generated from PB- and CB-derived HSCs. As shown in Fig. 6A, MCs generated from G-PBMC-derived $CD133^+$ HSCs showed 40-fold histamine release after IgE activation compared with controls. The histamine release after IgE activation was different among the cells generated from $CD133^+$ HSCs for all three cell sources. Fig. 6B shows the histamine content at Weeks 2, 4 and 8 with three different cell sources cultured in 3D. The data demonstrates that the histamine levels were below 1 pg/cell at Weeks 2 and 4 for the cells generated from $CD133^+$ HSCs all three cell sources. However, after eight weeks of culture, histamine levels increased significantly especially for the MCs generated from PB- and G-PBMC-derived $CD133^+$ HSCs.

3.1.7. Expression of cytokine and chemokine genes

RT-PCR was used to determine the expression of key chemokines and cytokines of the cells cultured in the tissue-engineered vascular model with fibroblast and ECs and the results are shown in Fig. 7.

Overall, the majority of the cytokine genes showed upregulation at Week 8 for MCs derived from all three cell sources. *PGD2* showed no upregulation until Week 8 for MCs generated from PB- and CB-derived $CD133^+$ HSCs. *MCP-1*, *GM-CSF* and *IL-8* were upregulated for MCs generated from all three cell sources at Week 2, 4 and 8. *MIP-1* was upregulated for MCs generated from derived from all three sources except MCs

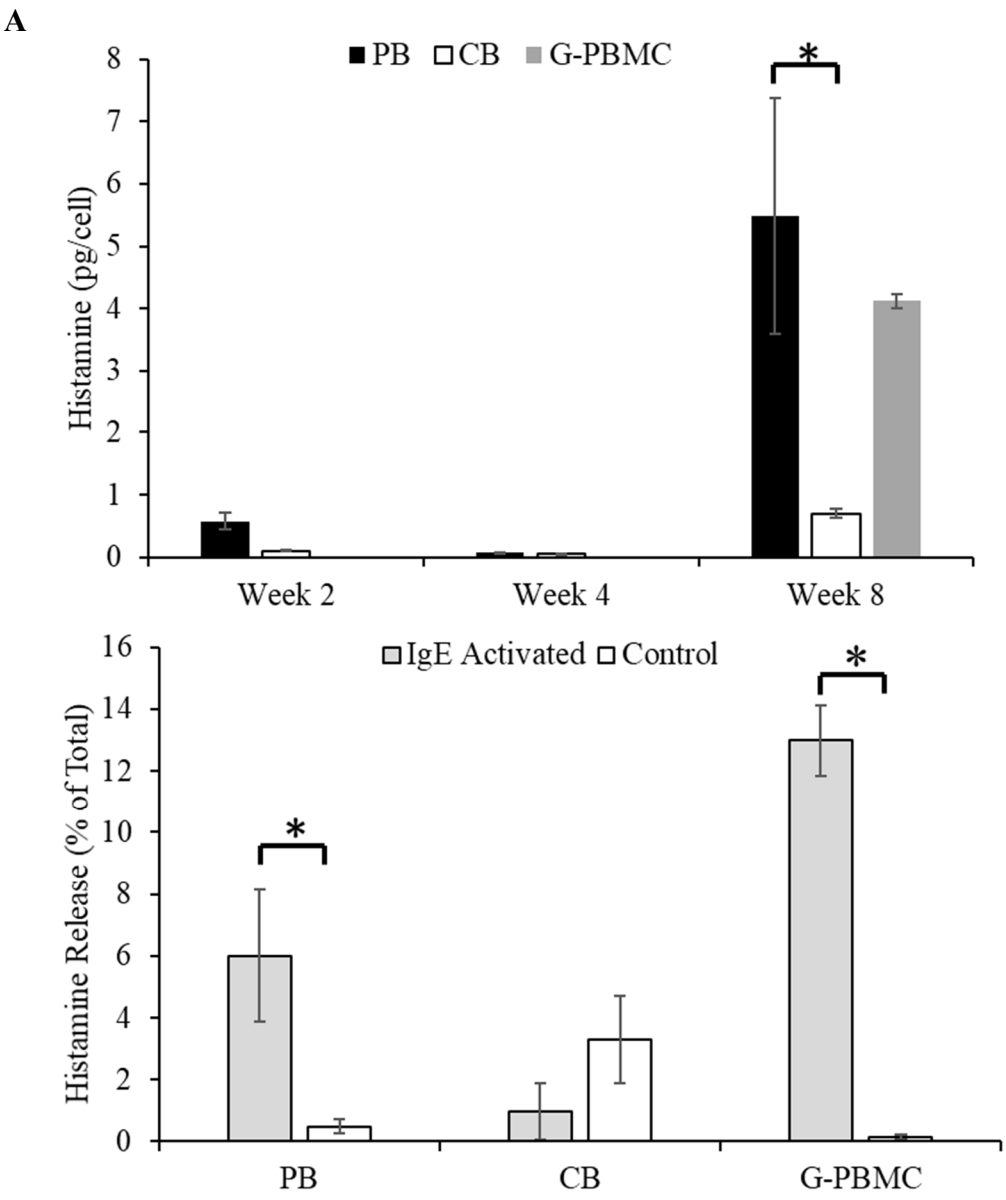

Figure 6. Histamine content and release from peripheral blood (PB)-, cord blood (CB)- and granulocyte colony-stimulating factor-mobilized peripheral blood mononuclear cells (G-PBMC)-derived cells in a 3D tissue-engineered vascular model with fibroblasts and endothelial cells. A) Histamine content was measured after two, four and eight weeks of culturing without IgE activation. B) Histamine release after immunoglobulin E (IgE) activation was measured after eight weeks of culture. Data are represented as mean ±SD; n=3. * indicates $p < 0.05$.

generated from PB- and CB-derived $CD133^+$ HSCs at Weeks 4 and 8, respectively. *TNF-α* was upregulated in MCs derived from PB and G-CSF and *IL-8* were upregulated for

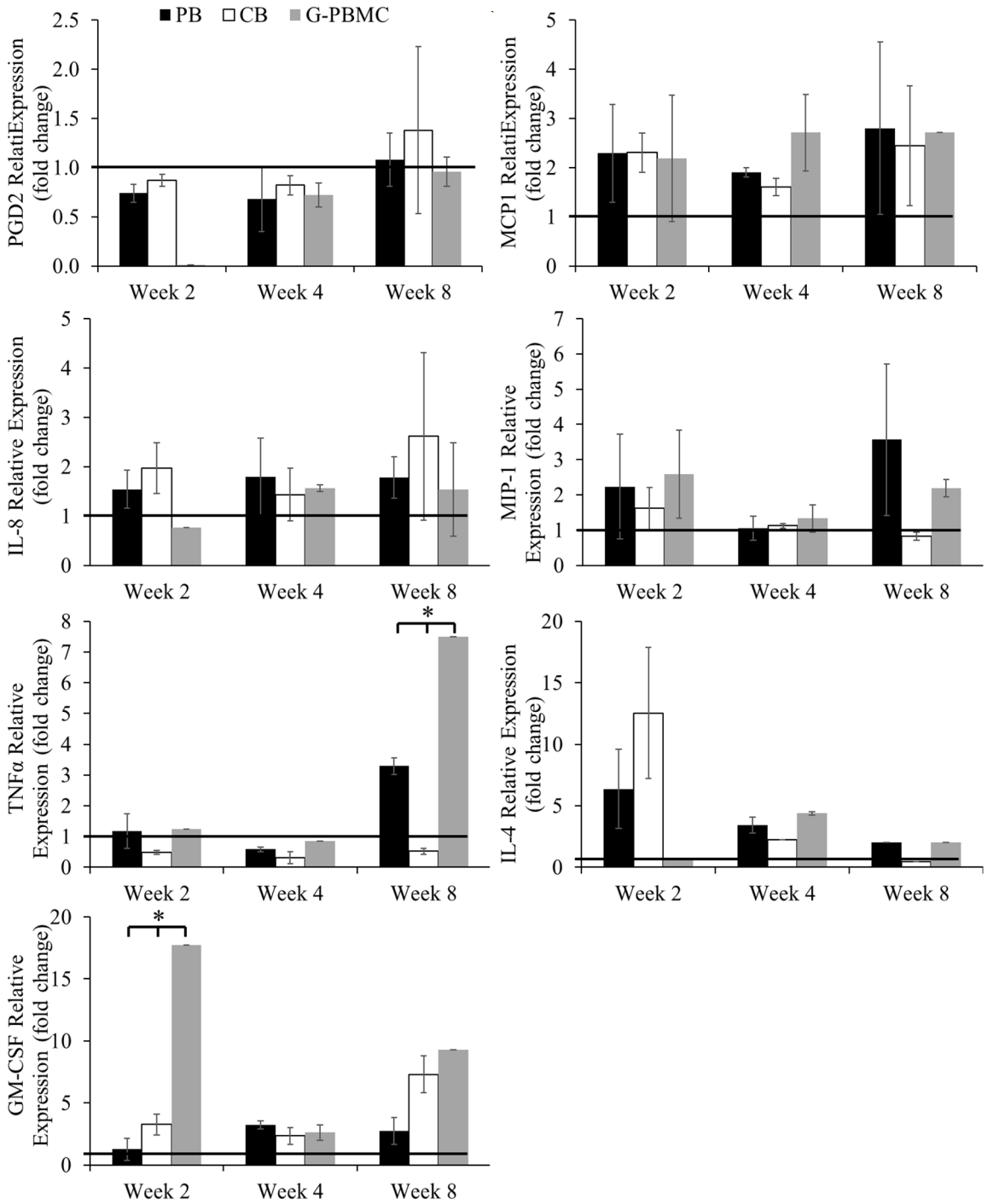

Figure 7. Fold increase in cytokine and chemokine genes in activated cells compared to and control cells from; human peripheral blood (PB)-, cord blood (CB)- and granulocyte colony-stimulating factor-mobilized peripheral blood mononuclear cells (G-PBMC)-derived $CD133^+$ cells in a 3D tissue-engineered vascular model with fibroblasts and endothelial cells. Activated cells were sensitized for 24h by the addition of monomeric immunoglobulin E (IgE) followed by crosslinking with anti-IgE receptors for 1h. Data are represented as mean ± SD; n=3. * indicates $p < 0.05$.

MCs generated from all three sources except MCs generated from PB- and CB-derived $CD133^+$ HSCs at Weeks 4 and 8, respectively.

TNF-α was upregulated in MCs derived from PB and G- PBMC sources at Week 8. *IL-4* expression was the highest in MCs generated from PB- and CB-derived $CD133^+$ HSCs at Week 2 but decreased afterward.

3.2. Determining the effect of fibroblasts and ECs on the growth and differentiation of MCs within the 3D tissue-engineered vascular model by comparing the generation of MCs from the 3D tissue-engineered vascular model to MCs from the 2D culture system

3.2.1. Cell density

Cell density increased in MCs generated from $CD133^+$ HSCs derived from three sources after 8 weeks of culture in the 3D tissue-engineered vascular model as well as 2D cell culture system (Fig. 8). The cell density increased from Week 2 and the cells from 3D and 2D cell culture systems started to form colonies. In both systems, the cell density increased with culture time.

3.2.2. Cell morphology

Morphological changes in cells derived from three sources in the 3D co-culture system and 2D cell culture system at Week 2, 4 and 8 were observed by metachromatic staining (Fig. 9). Mature MCs contained cytoplasmic granules that stained metachromatically with Wright-Giemsa. MCs derived from 3D and 2D cell culture models showed maturity with secretory granules stained blue or violet (Fig. 9).

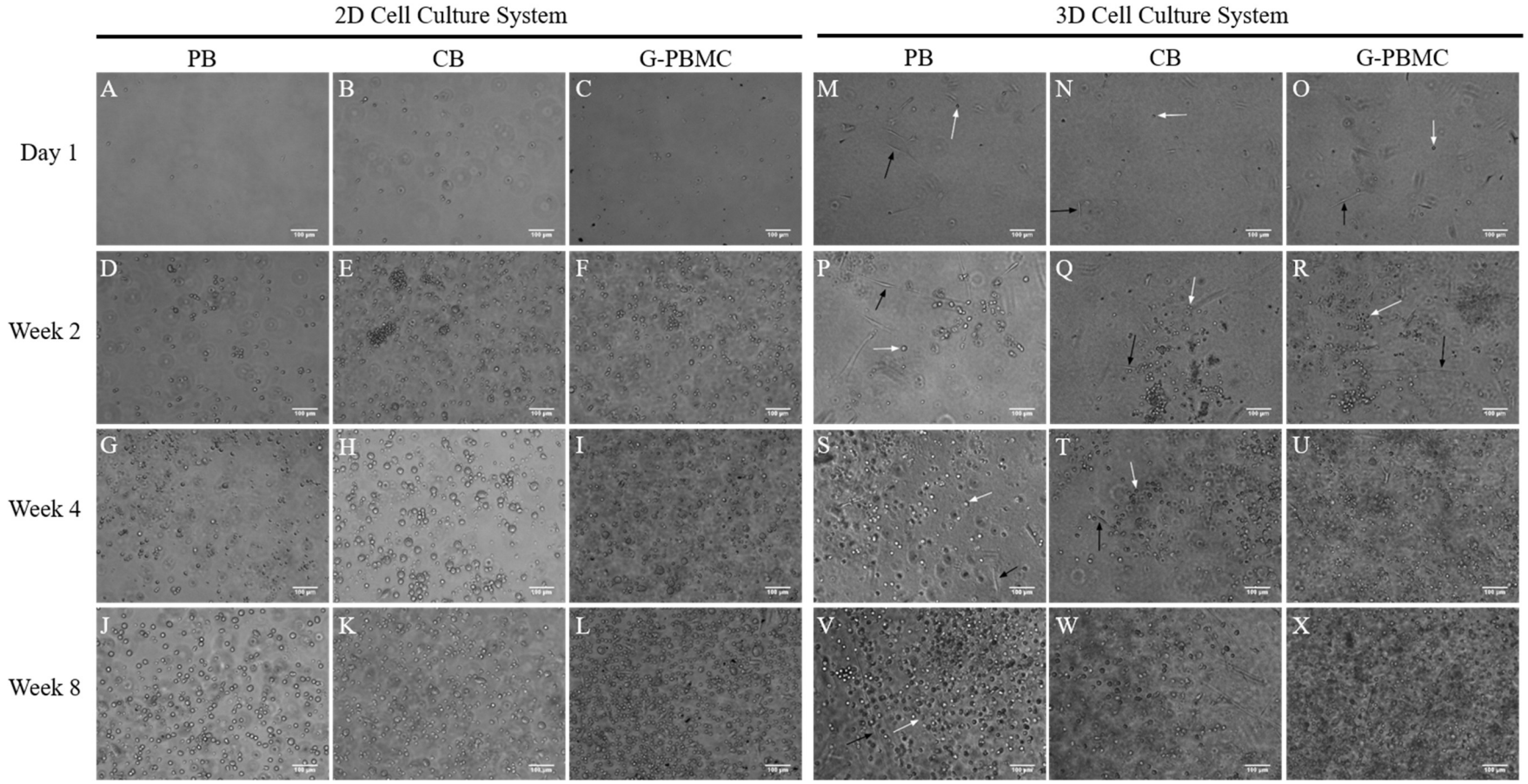

Figure 8. Increasing cell density for peripheral blood (PB)-, cord blood (CB)- and granulocyte colony-stimulating factor-mobilized peripheral blood mononuclear cells (G-PBMC)-derived cells over eight weeks in the 2D model without fibroblasts and endothelial cells (ECs) and 3D model with fibroblasts and ECs. Samples were examined by phase contrast microscopy once a week. Representative images are shown for triplicate samples of each group. White arrows point to typical mast cells (MCs). Black arrows point to typical fibroblasts. H, I) ECs were added to the cells at Week 8.

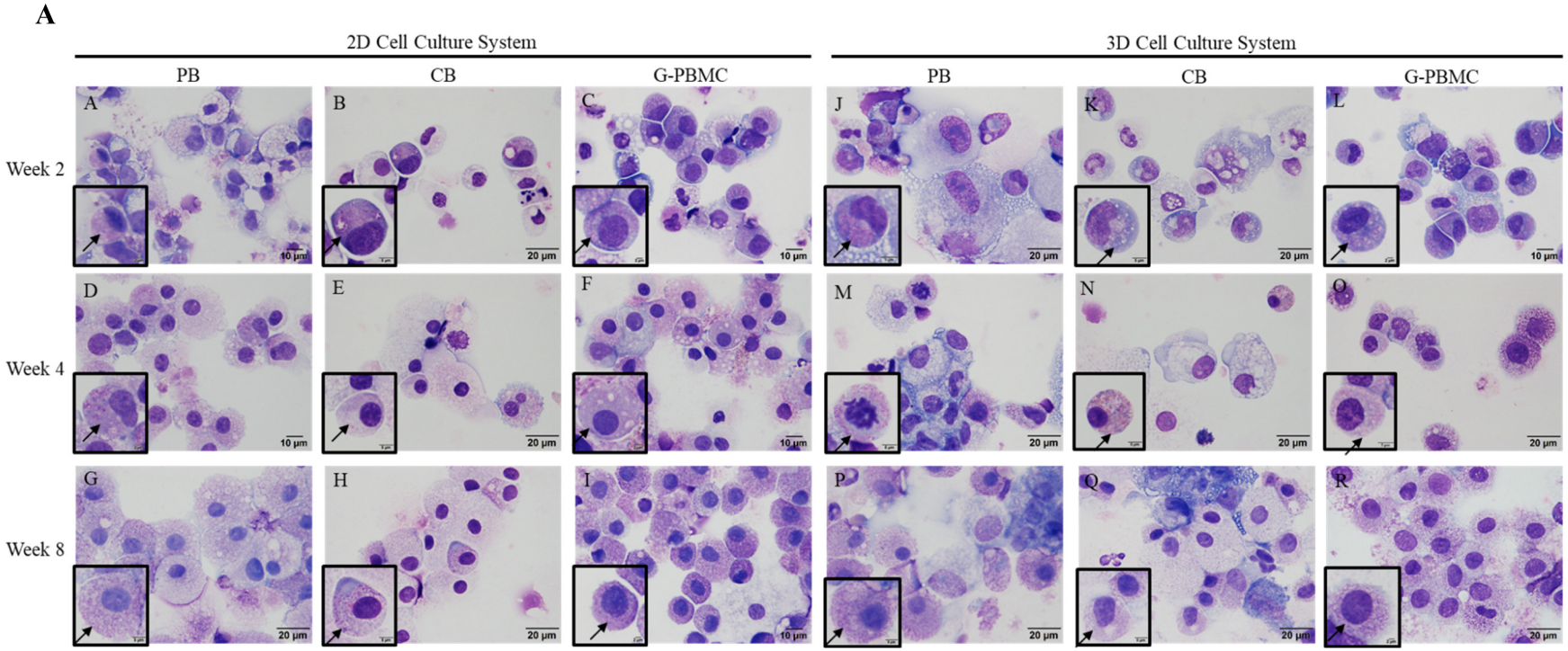
A
2D Cell Culture System
3D Cell Culture System
PB
CB
G-PBMC
PB
CB
G-PBMC
Week 2
Week 4
Week 8
A
B
C
J
K
L
D
E
F
M
N
O
G
H
I
P
Q
R
10 µm
20 µm

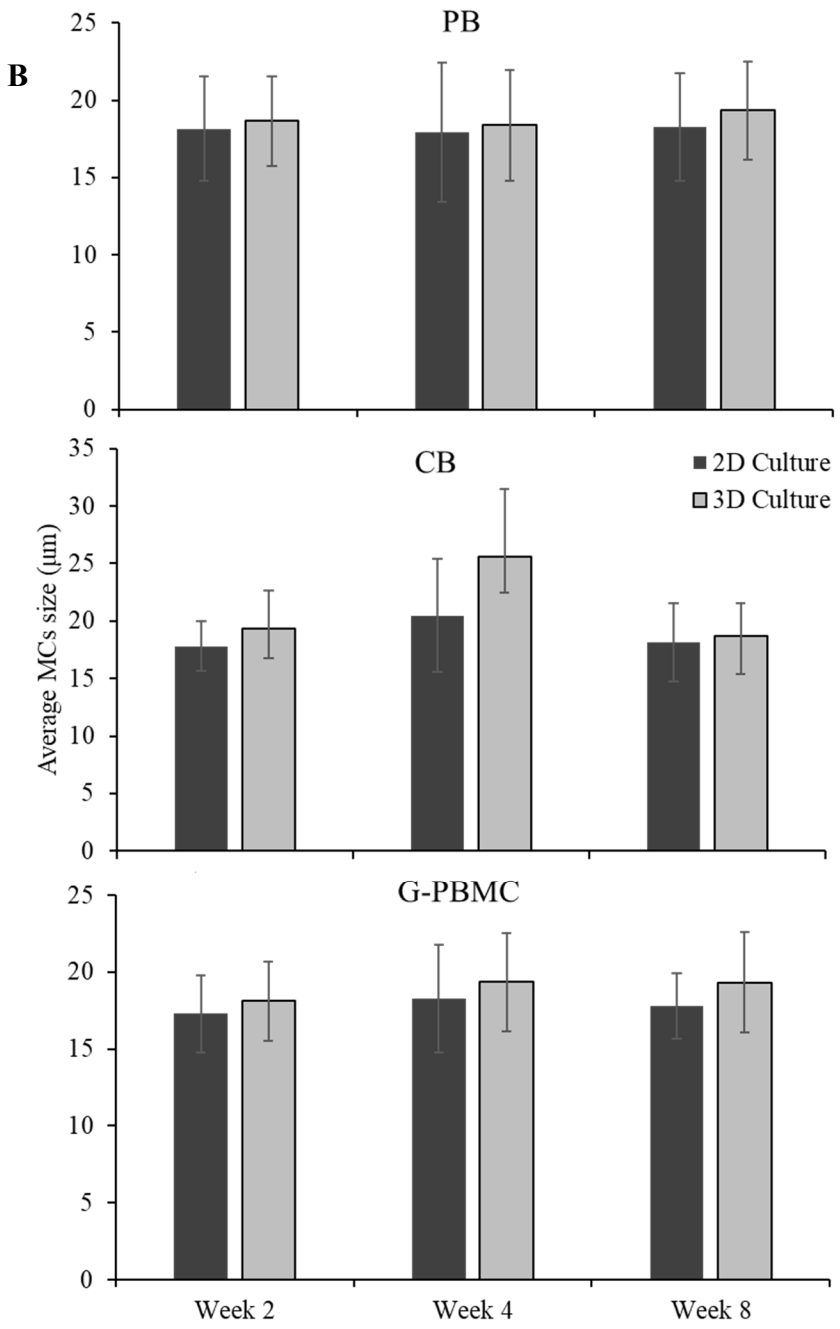

Figure 9. Morphological changes of peripheral blood (PB)-, cord blood (CB)- and granulocyte colony-stimulating factor-mobilized peripheral blood mononuclear cells (G-PBMC)-derived cells over eight weeks in a 2D model without fibroblasts and endothelial cells (ECs) and 3D culture system with fibroblasts and ECs. A) Cells were stained with Wright-Giemsa and examined by light microscopy. Representative images are shown for triplicate samples of each group. The granules of MCs stain a deep blue to violet. B) The average size of mast cells (MCs) after eight weeks of culture. Data are represented as mean ± SD; n=3.

The average MC sizes were very similar between the cell culture systems for three different cell sources. The cells generated from PB and CB were comparable. The average cell sizes for cells generated from G-PBMC were the smallest for both 2D and 3D culture systems.

A key difference between the two culture systems was that the 3D co-culture system showed a higher relative cell yield compared to the 2D system, especially for G-PBMC-derived $CD133^+$ HSCs. However, there was no significant difference in CB-derived cells between the two culture systems. In both 2D and 3D systems, PB- and G-PBMC-derived cells had the highest relative cell yield at Week 4, but decreased by Week 8.

3.2.3. Expression of FcεRI in c-kit^+ population

Cells that were cultured in the 3D co-culture system had a higher expression of FcεRI in the c-kit^+ population than the 2D model (Figs. 11). The FcεRI expression for c-kit^+ cells generated from CB-derived $CD133^+$ HSCs at Week 4 and Week 8 was comparable between the two culture systems. In contrast, the c-kit^+ cells generated from PB- and G-PBMC-derived $CD133^+$ HSCs had a higher expression of FcεRI in the 3D culture, when compared to 2D cultures at Weeks 2 and 4. This data indicated that the 3D tissue-engineered vascular model with fibroblasts and ECs were able to generate MCs with FcεRI expression in c-kit^+ population.

3.2.4. Expression of tryptase and chymase

MCs generated from PB- and G-PBMC-derived $CD133^+$ HSCs showed a high expression (>90%) of tryptase and chymase in both 2D and 3D culture systems (Figs. 12B, C). Interestingly, in 2D cultures, the tryptase expression increased over time in MCs

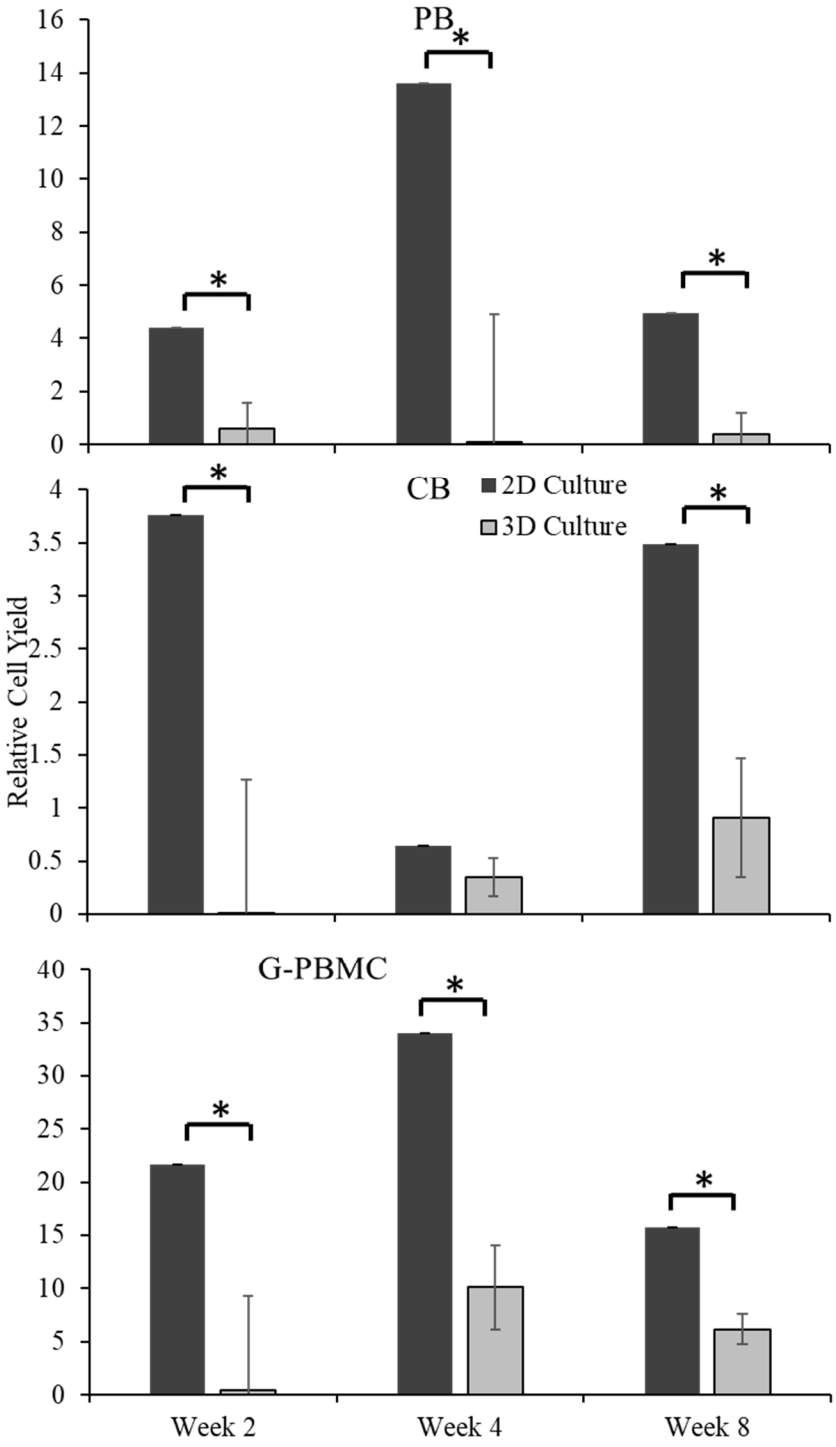

Figure 10. Relative cell yield from peripheral blood (PB)-, cord blood (CB)- and granulocyte colony-stimulating factor-mobilized peripheral blood mononuclear cells (G-PBMC)-derived $CD133^+$ progenitor cells during eight weeks of culture in a 2D model without fibroblasts and endothelial (ECs) and a 3D culture model with fibroblasts and ECs. Data are represented as mean ± SD; n=3. * indicates $p < 0.05$.

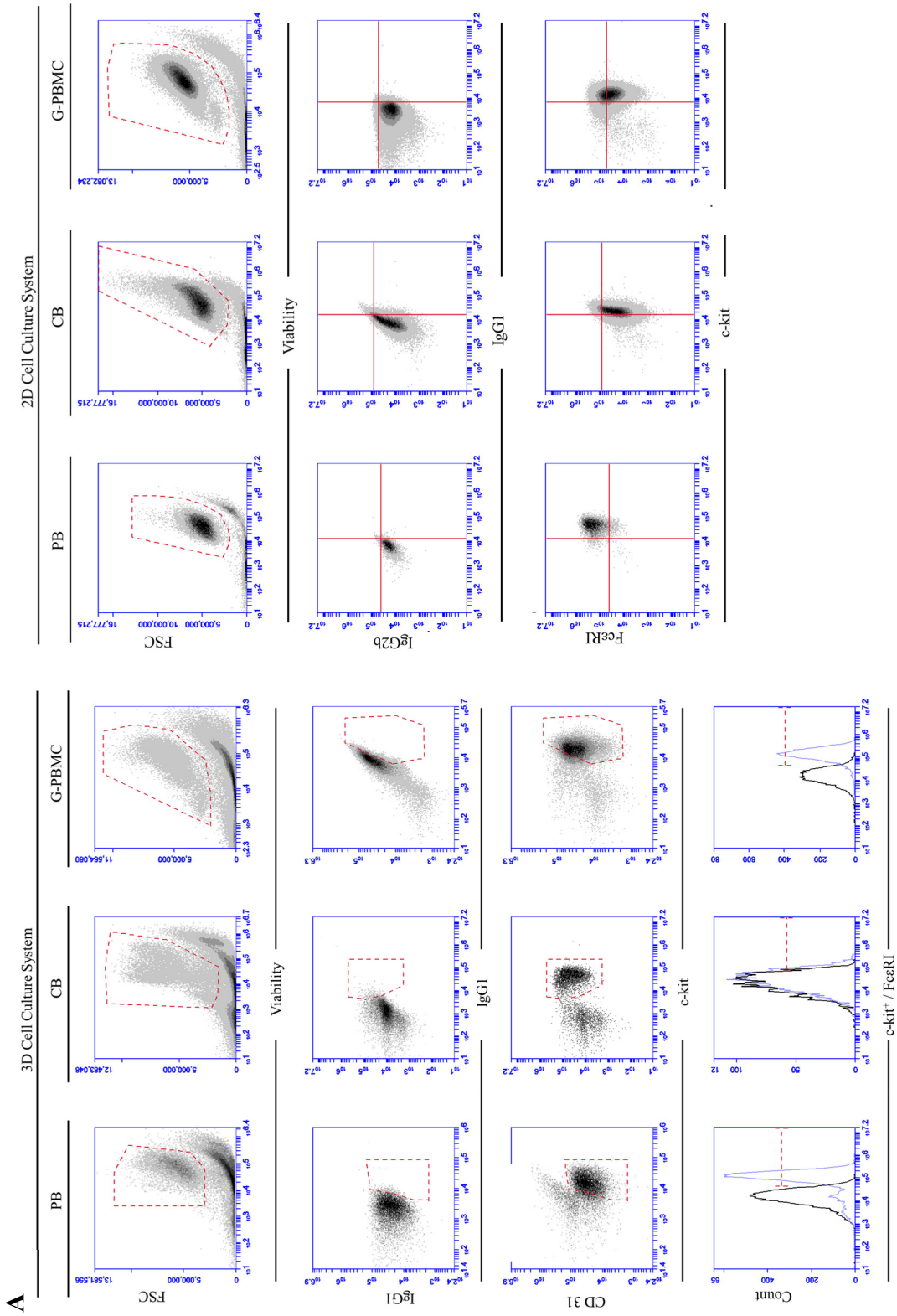
A
3D Cell Culture System
PB
CB
G-PBMC
FSC
Viability
IgG1
CD 31
c-kit
Count
c-kit+ / FcεRI
2D Cell Culture System
PB
CB
G-PBMC
FSC
Viability
IgG2b
IgG1
FcεRI
c-kit

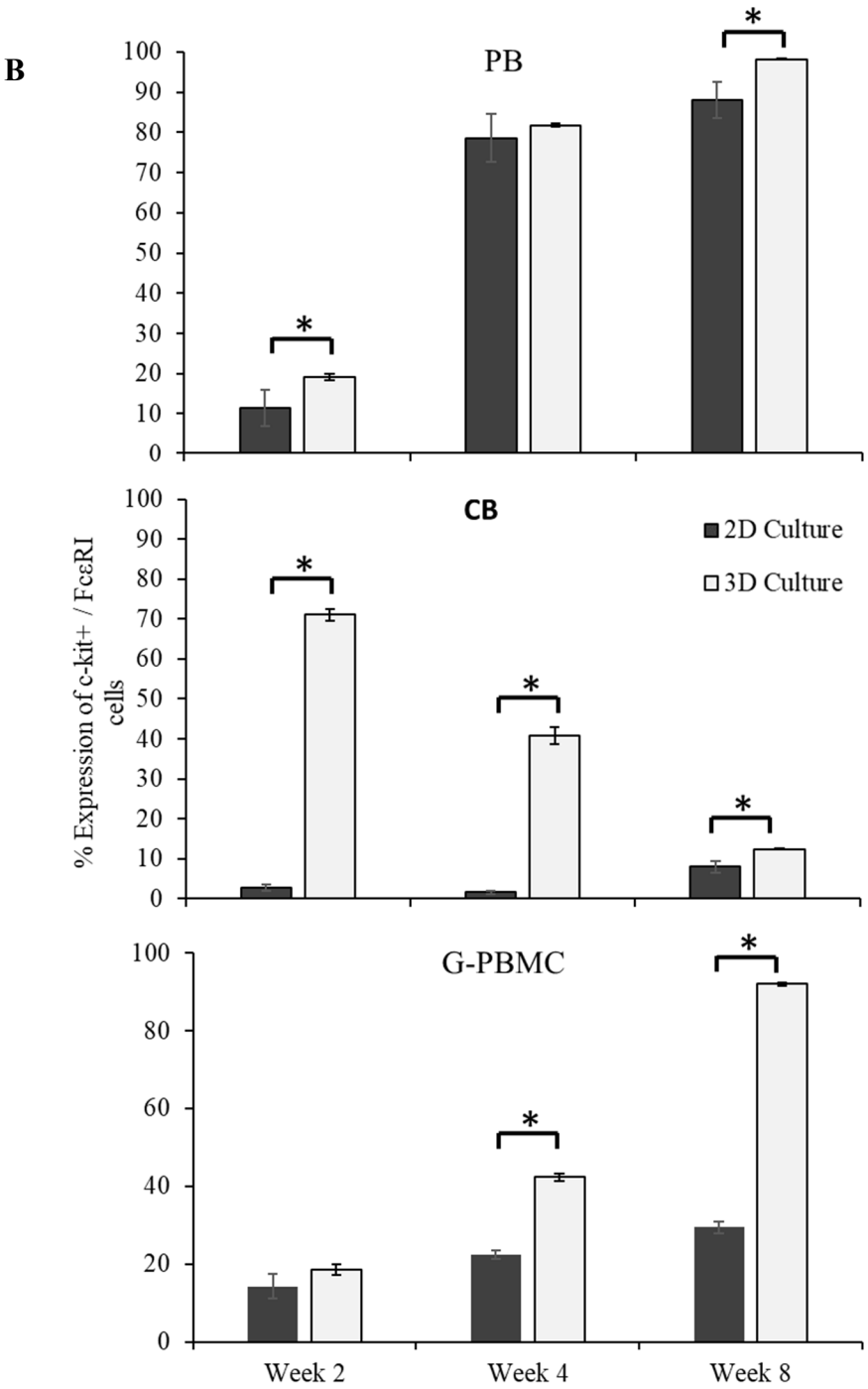

Figure 11. Expression ofc-kit^{+}/ FcεRI^{+} from peripheral blood (PB)-, cord blood (CB)- and granulocyte colony-stimulating factor-mobilized peripheral blood mononuclear cells (G-PBMC)-derived CD133^{+} progenitor cells during eight weeks of culture. A) The gating scheme and representative density plots of the expression of phenotypic markers using flow cytometry. B) The bar graphs show the percentage of c-kit^{+}/ FcεRI^{+}expression. Data are represented as mean ±SD; n=3. * indicates $p < 0.05$.

generated from PB-derived HSCs (Figs. 12). However, in the 3D cultures, tryptase expression by these cells increased after an initial decrease. The cells generated from CB-derived $CD133^+$ HSCs had higher tryptase expression at Week 8 in the 3D co-culture system compared to the 2D system. The expression of chymase in cells generated from PB- and G-PBMC-derived $CD133^+$ HSCs steadily increased in 2D cell culture system.

Our results showed that both the 3D and 2D systems could generate mature MCs. However, only the 3D system could generate MCs with >80% tryptase expression from all three sources.

3.2.5. Histamine content and release

The cells generated from PB-, CB- and G-PBMC-derived $CD133^+$ HSCs produced histamine in both 2D and 3D culture systems (Figs. 12). The $CD133^+$ HSCs generated from the 3D culture model displayed a measurable histamine content. For histamine release and histamine content, cells generated from PB and CB at the 2D system had a higher histamine release level than the 3D culture mode. The cells generated from G-PBMC had a higher histamine content and release level when cultured in the 3D culture system than in 2D culture system.

3.2.6. Expression of cytokine and chemokine genes

To determine if the soluble factors from the fibroblasts and ECs within the 3D culture system contribute to MC growth and differentiation, the levels of the cytokines and chemokines from the 2D and 3D systems were measured (Fig. 14). Histamine was measured for the cells generated from the G-PBMC at Week 2 and 4 but the values were

below the range of the analysis. In the 2D culture system, more cytokine genes were upregulated compared to the 3D co-culture system with fibroblasts and ECs (Fig. 14). All the cytokine genes showed upregulation for cells generated from PB and CB in the 2D culture system.

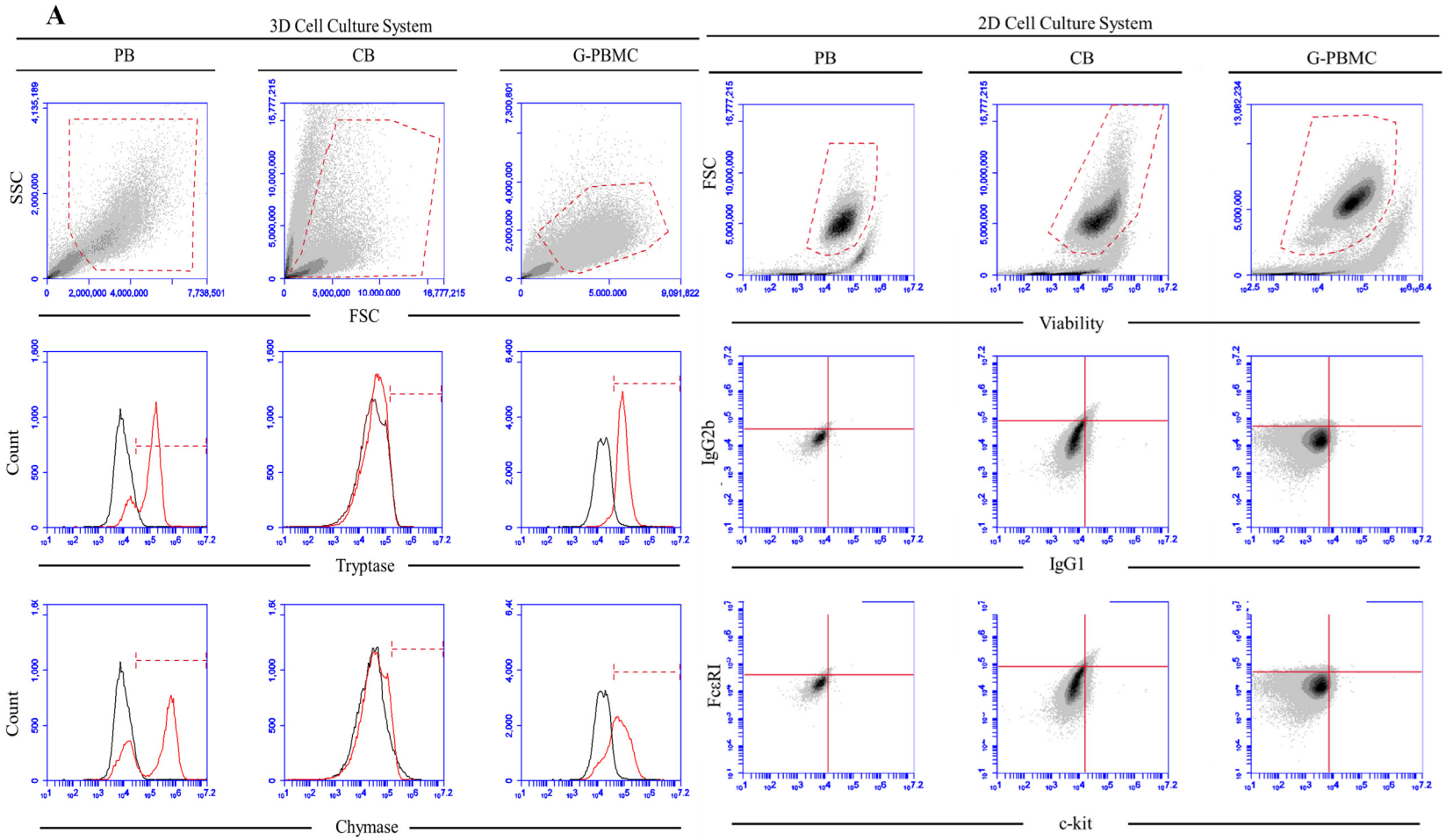
A
3D Cell Culture System
2D Cell Culture System
PB
CB
G-PBMC
PB
CB
G-PBMC
SSC
FSC
FSC
Viability
Count
Tryptase
IgG2b
IgG1
Count
Chymase
FcεRI
c-kit

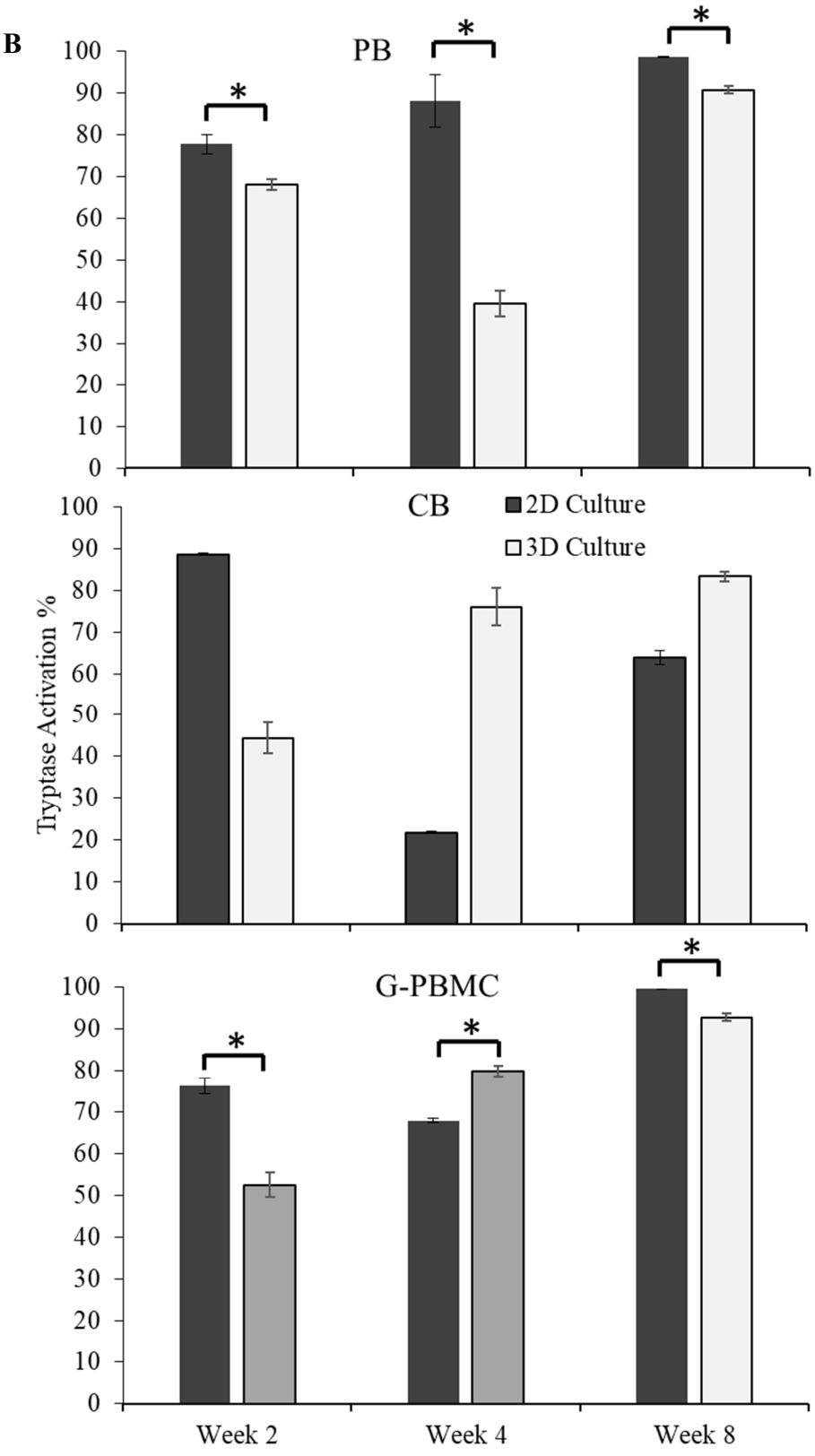
B
PB
CB
G-PBMC
2D Culture
3D Culture
Tryptase Activation %
Week 2
Week 4
Week 8
*

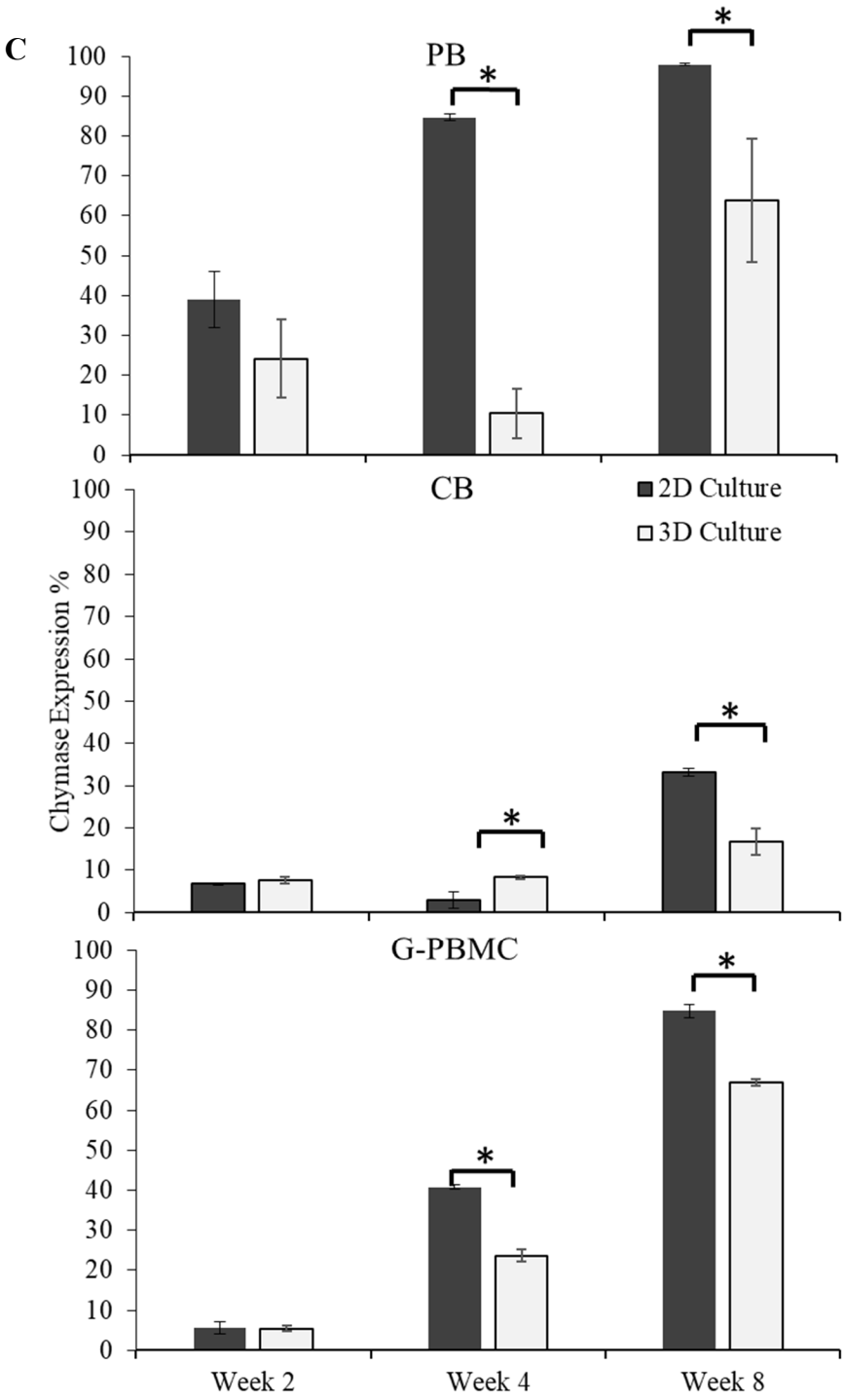

Figure 12. Expression of tryptase and chymase in cells differentiated from peripheral blood (PB)-, cord blood (CB)- and granulocyte colony-stimulating factor-mobilized peripheral blood mononuclear cells (G-PBMC)-derived $CD133^{+}$ progenitor cells after eight weeks in a 3D co-culture system and 2D culture system without fibroblasts and ECs. A) The gating strategy to identify tryptase and chymase population; percentage of B) tryptase and C) chymase expression. Data are represented as mean ± SD; n=3. * indicates $p < 0.05$. Data are represented as mean ±SD; n=3. * indicates $p < 0.05$.

A

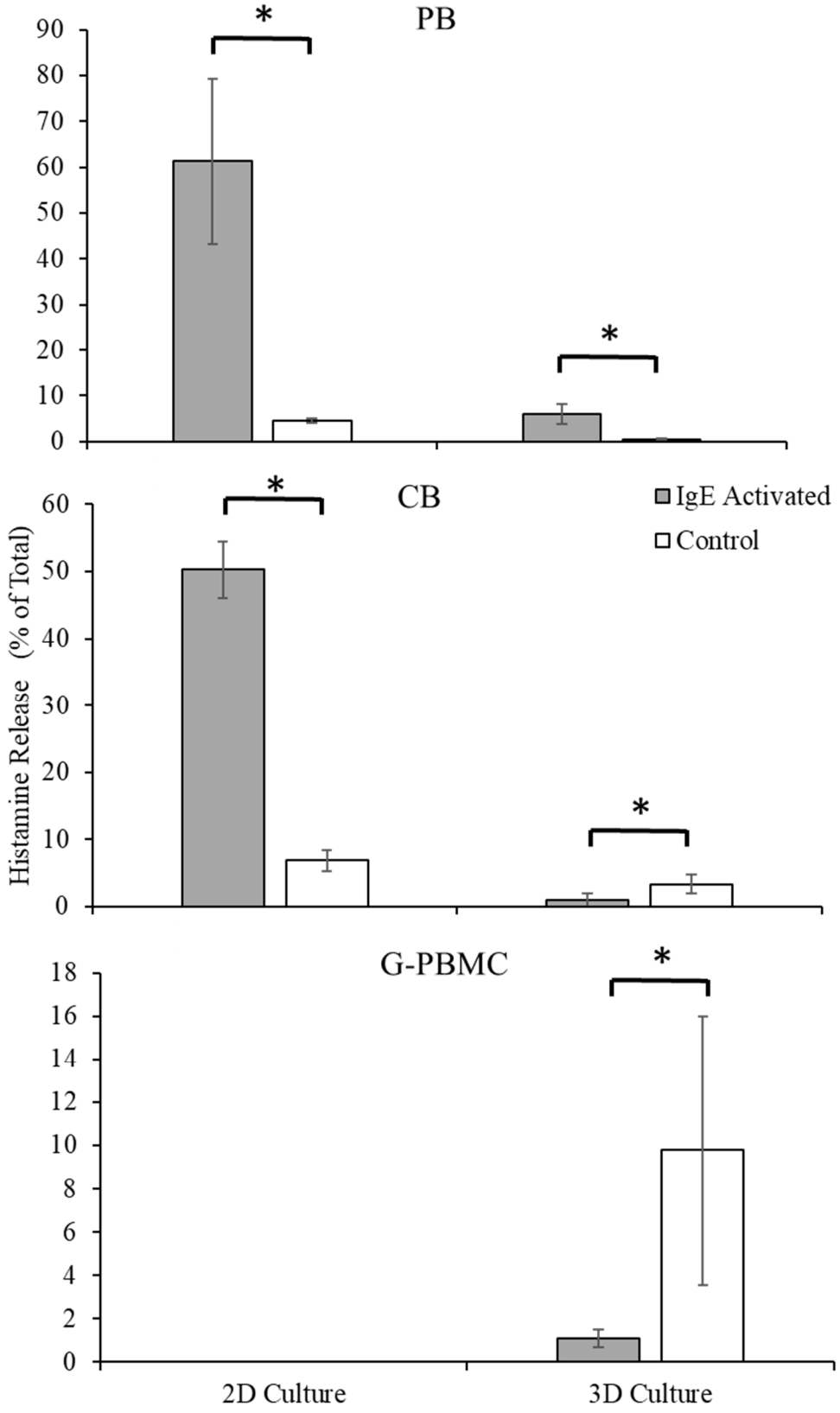
PB
CB
G-PBMC
IgE Activated
Control
Histamine Release (% of Total)
2D Culture
3D Culture
*

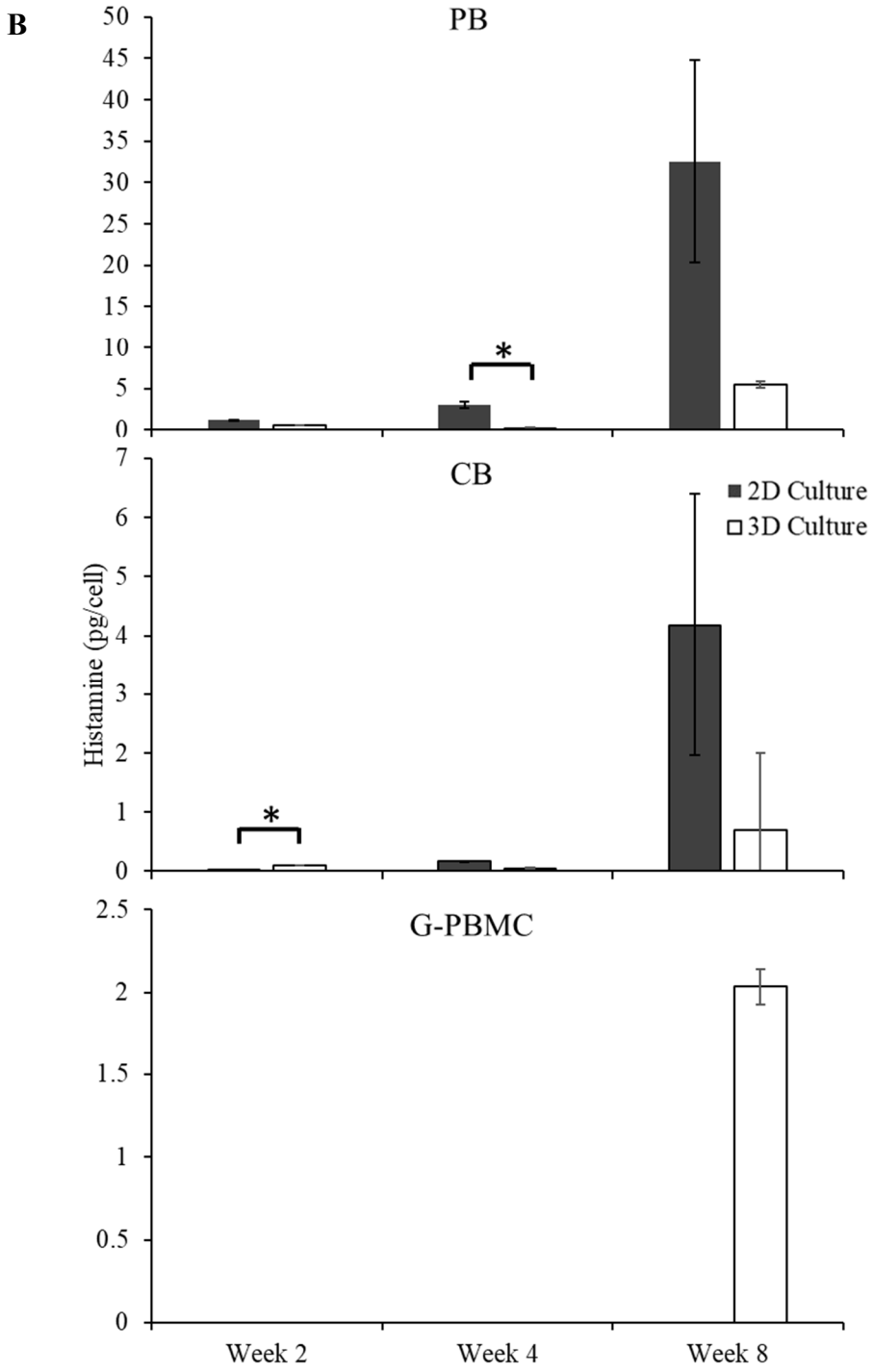

Figure 13. Histamine content and release from peripheral blood (PB)-, cord blood (CB)- and granulocyte colony-stimulating factor-mobilized peripheral blood mononuclear cells (G-PBMC)-derived cells in a 2D cell culture model without fibroblasts and endothelial cells (ECs) and a 3D tissue-engineered vascular model with fibroblasts and ECs. A) Histamine was measured after two, four and eight weeks of culturing without immunoglobulin E (IgE) activation. B) Histamine release was measured after eight weeks of culture. Data are represented as mean ±SD; n=3. * indicates $p < 0.05$.

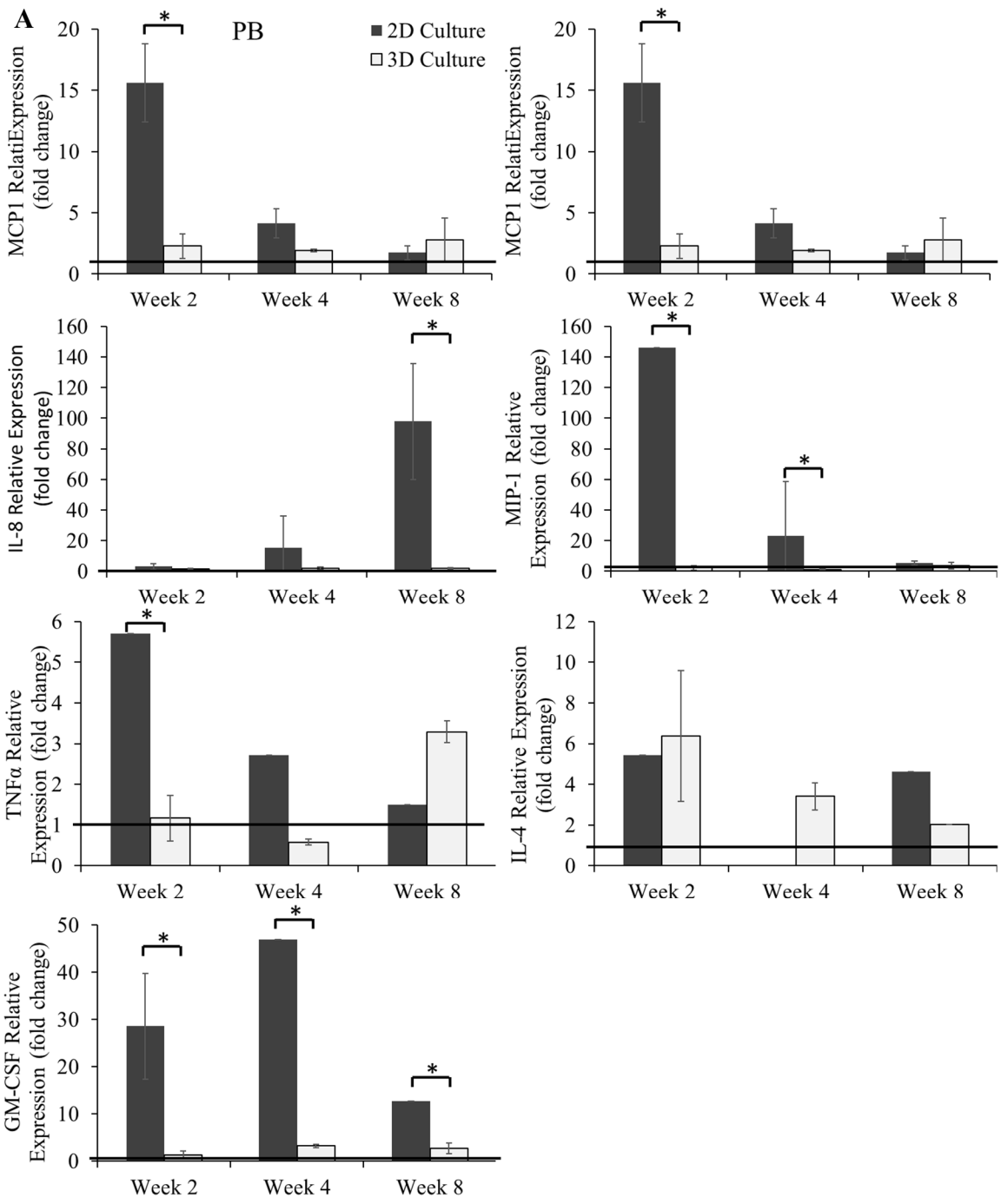
A
PB
2D Culture
3D Culture
MCP1 RelatiExpression (fold change)
MCP1 RelatiExpression (fold change)
IL-8 Relative Expression (fold change)
MIP-1 Relative Expression (fold change)
TNFα Relative Expression (fold change)
IL-4 Relative Expression (fold change)
GM-CSF Relative Expression (fold change)
Week 2
Week 4
Week 8
*

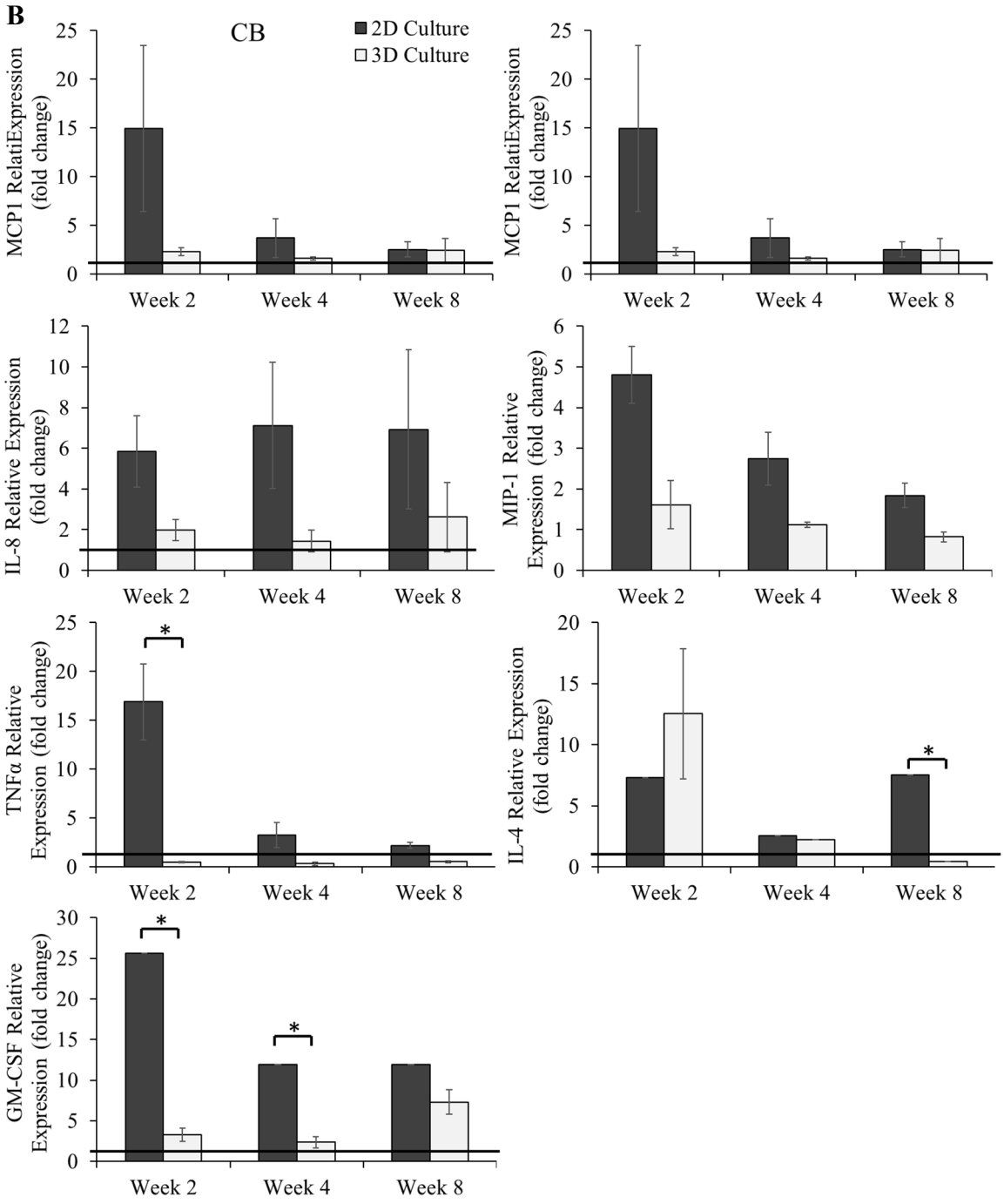
B
CB
2D Culture
3D Culture
MCP1 RelatiExpression (fold change)
MCP1 RelatiExpression (fold change)
IL-8 Relative Expression (fold change)
MIP-1 Relative Expression (fold change)
TNFα Relative Expression (fold change)
IL-4 Relative Expression (fold change)
GM-CSF Relative Expression (fold change)
Week 2
Week 4
Week 8
*

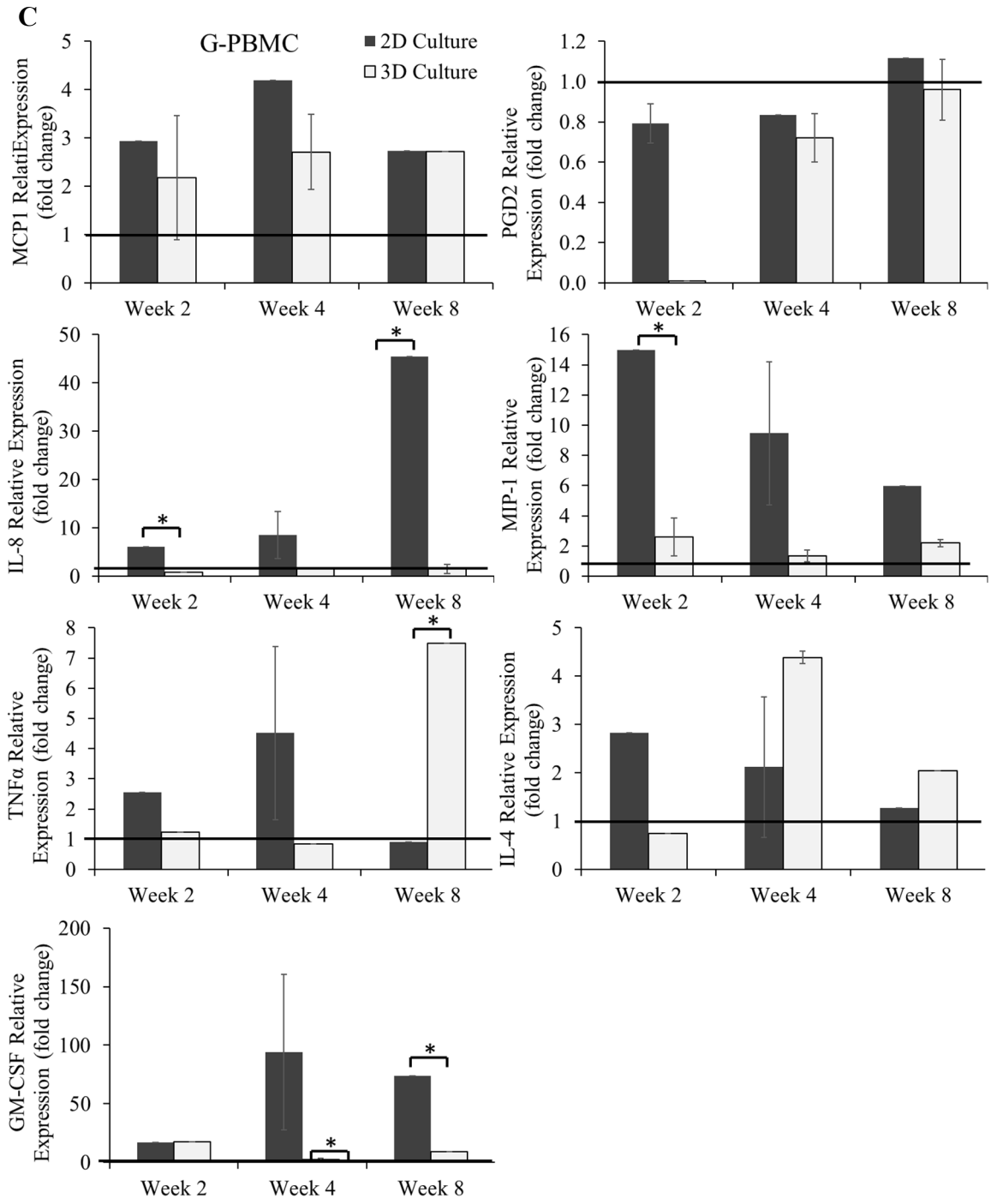

Figure 14. Fold increase in cytokine and chemokine genes in activated and control cell differentiated from human A) peripheral blood (PB)-, B) cord blood (CB)- and C) granulocyte colony-stimulating factor-mobilized peripheral blood mononuclear cells (G-PBMC)-derived $CD133^+$ cells in a 2D cell culture system without fibroblasts and endothelial cells (ECs) and a 3D tissue-engineered vascular model with fibroblasts and ECs. Activated cells were sensitized for 24h by the addition of monomeric immunoglobulin E (IgE) followed by crosslinking with anti-IgE receptors for 1h. Data are represented as mean ±SD; n=3. * indicates $p < 0.05$.

CHAPTER IV

DISCUSSION

4.1. Identifying which source of adult human CD133+ hematopoietic stem cells generates the greatest number of viable and mature MCs within a 3D tissue-engineered vascular model.

4.1.1. Cell proliferation and morphology

The cells generated from peripheral blood (PB)-, cord blood (CB)- and granulocyte colony-stimulating factor-mobilized peripheral blood mononuclear cell (G-PBMC) started to form colonies, which is a key characteristic for MCs [57]. Microscopy images showed the cell concentrations increasing with culture period (Fig. 1). It was difficult to differentiate the proliferation and cell numbers between three cell sources solely based on phase contrast microscopy images. Hence Wright-Giemsa stain was used to determine the cell proliferation and cell numbers (Fig. 2).

Studies have shown that MCs are round in shape, while fibroblasts are elongated when co-cultured in collagen [58]. ECs are cobblestone in appearance, and sometimes form incomplete loops when co-cultured with MCs [59]. MCs are 10-20 μm in size and have round nuclei but studies have suggested with continued growth of granules, MCs can reach 20-30 μm in diameter [60-62]. A key feature of MCs are the granules which stain

purple and violet following metachromatic staining [63, 64]. Approximately 50% of the cytoplasm of mature MCs are filled with granules [65]. MC differentiation is involved in different pathological and physiological processes through direct cell-cell interactions or the release of mediators [66]. Studies have shown that when MCs are cultured in loose connective tissue environment, MCs are more likely to become round in shape, however, when MCs are cultured in close contact with blood vessels, MCs appear ovoid or elongated. Furthermore, when MCs are cultured in dermal fibers, they become spindle-shaped or threadlike. It is usual for MCs to have more than one nucleus [62]. The cells generated from $CD133^+$ HSCs from three different sources grown in the 3D tissue-engineered vascular model with fibroblasts and ECs showed signs of maturity with secretory granules stained blue or violet (Fig. 2).

The cells generated from G-PBMC-derived $CD133^+$ HSCs showed an average of 1.5-fold cell yield compared with other cell sources. As shown in Figs. 1 – 3, phase contrast microscopy and Wright-Giemsa images support the relative cell yield calculation. G-PBMC-derived progenitor cells had the highest relative cell yield compared with cells generated from PB- and CB-derived $CD133^+$ HSCs in 3D tissue-engineered vascular model with fibroblasts and ECs.

Researchers have shown G-PBMC had a significant reduction in the proportion of apoptotic cells in the progenitor cells population compared to unstimulated PB-derived progenitor cells [67-70]. This might explain the high relative cell yield and MCs ratio from cells generated from G-PBMC but firm conclusions on the exact effect on granulocyte colony-stimulating factor (G-SCF) remains to be established.

4.1.2. Expression of FcεRI in c-kit$^+$ population

FcεRI is a high-affinity IgE receptor, essential for the induction of IgE-mediated allergic reactions. Cross-linking of cell surface FcεRI begin with IgE binding with antigens. This is followed by MC degranulation and the release of different inflammatory mediators that provoke allergic inflammation. However, many studies have shown that MCs lack FcεRI both *in vivo* and *in vitro* conditions [45, 71]. Researchers have shown that almost two-thirds of MCs cultured from normal human dermis expressed faint to no FcεRI using dual-color immunohistochemical staining [72]. Other studies have reported FcεRI expression had a range of 30-40% in PB- and CB-generated cells [45]. Taken together, the data indicate that CB-derived HSCs was not a suitable source for generating c-kit$^+$/FcεRI$^+$ MCs.

A major difference between PB/G-PBMC and CB is their abilities in the number and type of differentiated cell types they can differentiate. CB stem cells are pluripotent and can become all cell types. PB stem cells are limited to differentiating into different cell types.

4.1.3. Expression of MCs mediators

When a specific allergen, cytokines, or immunoglobulin E (IgE) triggers MCs through high-affinity surface IgE receptors and FcεRI cross-linking, this causes MC activation and release of a range of rapid inflammation mediators from MC granules, such as histamine, neutral proteases like tryptase and chymase, cytokines, chemokines and many proteases that rapidly interact with connective tissue, vasculature and inflammatory cells within minutes [73]. The two MC subtypes that have been discovered in tissue include the MCs where the granules contain only protease tryptase (MC_T) or where the granules

contain both tryptase and chymase (MC_{TC}). The cells generated from three cell sources had over 80% tryptase expression.

The histamine content and release were examined to determine the functionality of MCs. In the 3D culture system, the cells generated from G-PBMC-derived $CD133^+$ HSCs showed the highest histamine content compared with cells generated from PB- and CB-derived HSCs. This might relate to G-CSF stimulates the development of MCs progenitor cells [70, 74].

IgE activation cause MCs to produce a range of pro-inflammatory mediators including multiple cytokines and chemokines [75, 76]. Of these, PGD2, MCP-1, IL-8, MIP-1, TNF-α, IL-4 and GM-CSF are of pathological significance for mature MCs [77]. When an IgE triggers MCs through high-affinity surface IgE receptors and FcεRI cross-linking, MCs are activated and release a range of rapid inflammation mediators, such as cytokines, chemokines and many proteases that rapidly interact with connective tissue, vasculature and inflammatory cells [73]. These mediators have an intense effect on surrounding tissues and can cause a broad range of cellular responses, including tumorigenesis [78]. The molecular mechanisms and relationship between MCs and co-stimulatory molecules remain unclear. TNF-α is a common cell signaling protein that included in different pathological states and it is important to study its impact on MCs in regulating immune responses [79, 80]. Mature MC is known for its expression of GM-CSF receptors [81]. MCP-1 and IL-8 are common chemokines and their productions can indicate the maturity of MCs after the activation [82]. However, further studies for the

MCs cytokine expression and production are needed to fully understand the exact mechanisms.

4.2. Determining the effect of fibroblasts and ECs on the growth and differentiation of MCs within the 3D tissue-engineered vascular model by comparing the generation of MCs from the 3D tissue-engineered vascular model to MCs from the 2D culture system

4.2.1. Cell proliferation and morphology

The comparison of cell density from cells generated from PB, CB and G-PBMC were cultured in 3D tissue-engineered vascular model and 2D traditional cell culture system shown the microscopy images were indistinguishable. Fig. 8 shown cells were started to form colonies at Week 2, which is a key characteristic for MCs.

Wright-Giemsa were used to stain the cells and investigated the morphology of the cells that were cultured in the two cell culture systems. The generated cells from both cell culture systems shown signs of maturity with secretory granules stained blue or violet (Fig.9).

The cells generated from PB and G-PBMC had a higher relative cell yield than CB. It might indicate the adult stem cell type are different than CB-derived progenitor cells.

Regardless, results from the morphology and cell proliferation experiments demonstrated that the 3D co-culture systems had the ability to differentiate MCs from $CD133^{+}$ hematopoietic stem cells (HSC).

4.2.2. Expression of FcεRI in c-kit^{+} population

The cells generated from the 3D co-culture system had a higher FcεRI expression compared to the 2D cell culture system. This result indicated the possibility of fibroblast and ECs stimulating the growth of MCs from HSC in the 3D tissue-engineered vascular model.

4.2.3. Expression of MC mediators

The cells cultured in both 2D and 3D cell culture systems from three cell sources shown tryptase and chymase expression. It is possible that for the tryptase and chymase expressions, fibroblasts and ECs has a limited effect on the progenitor cells differentiated MCs.

The cells cultured in both 2D and 3D cell culture systems from three cell sources showed detectable histamine content and release when activated. In order to trigger 3D cultured MCs through IgE receptors and FcεRI cross-linking, IgE and anti-IgE were added directly on top of the collagen gel. This could cause the release of histamine; however, the released histamine might get trapped in the collagen gel. As the IgE and anti-IgE were not directly in contact with the cells in the 3D culture system, it could affect the histamine levels. It might also explain the higher levels of histamine in PB- and CB-generated cells in the 2D culture system.

The cells cultured in the 3D and 2D culture systems showed upregulated expression of the majority of cytokine and chemokine genes.

CHAPTER V

CONCLUSIONS

Allergic diseases have increased dramatically in many nations and mast cells are key effector cells in the allergic inflammatory response. MCs do not circulate but remain relatively fixed and dispersed in tissues and it is difficult to isolate high numbers of viable and mature cells. Due to the traditional 2D environment cannot completely recapitulate the organized cellular structure of tissues *in vivo*, it is important to develop an *in vivo* microenvironment that mimics the human tissue layer.

PB-, CB- and G-PBMC-derived progenitor cells were cultured in a 3D tissue-engineered vascular model with FCs and ECs for eight weeks to determine which sources provided the highest number of viable and mature MCs. After comparing the morphology, proliferation, FcεRI in the c-kit$^+$ population, tryptase and chymase expression, histamine levels, and cytokine and chemokine expression, It was determined that G-PBMC-derived progenitor cells generate the greatest number of viable and mature MCs within a 3D tissue-engineered vascular model based on the result showed that G-PBMC had the highest proliferation rate and tryptase and chymase expression, a high FcεRI expression in the c-kit$^+$ population and histamine level.

Comparing to cells grown in the 2D system without FCs and ECs, the 3D tissue-engineered vascular model with FCs and ECs generated a greater number of mature MCs based on the result showed that 3D cell culture system had the highest proliferation rate and FcεRI expression in the c-kit^{+} population, high level of tryptase and chymase expression and histamine level. This result suggests that fibroblasts and ECs may contribute to the growth and differentiation of MCs. Even though the 3D co-culture system generated a greater number of viable and mature MCs, we believe that the system still needs to be optimized. The protocol for this new culture system was based on a protocol for standard 2D cell culture. Therefore, the distinct differences between the two systems, such as a co-culture within a 3D matrix, should be taken into account to optimize the 3D system.

In conclusion, these results indicate that the tissue-engineered vascular model can be used to develop MCs from various stem cell sources and that the cells may be more functional than those developed in 2D cell culture systems, due to the influence of fibroblasts and ECs. These results highlight the possibility of using the tissue-engineered vascular model to culture functional MCs for future study and testing of allergy and other MC-related diseases.

REFERENCES

1. *Chronic diseases: a 21st century epidemic* July - August 2009. **8**(4).
2. Arbes, S.J., et al., *Prevalences of positive skin test responses to 10 common allergens in the US population: results from the third National Health and Nutrition Examination Survey.* Journal of Allergy and Clinical Immunology, 2005. **116**(2): p. 377-383.
3. Gebhardt, T., et al., *Cultured human intestinal mast cells express functional IL-3 receptors and respond to IL-3 by enhancing growth and IgE receptor-dependent mediator release.* European journal of immunology, 2002. **32**(8): p. 2308-2316.
4. Saito, H., *Mast cell-specific genes–new drug targets/pathogenesis*, in *Mast Cells in Allergic Diseases*. 2005, Karger Publishers. p. 198-212.
5. Persson, C.G., *Mice are not a good model of human airway disease.* American journal of respiratory and critical care medicine, 2002. **166**(1): p. 6-7.
6. Kocabas, C.N., et al., *Analysis of the lineage relationship between mast cells and basophils using the c-kit D816V mutation as a biologic signature.* Journal of allergy and clinical immunology, 2005. **115**(6): p. 1155-1161.
7. Marshall, J.S., *Mast-cell responses to pathogens.* Nature Reviews Immunology, 2004. **4**(10): p. 787.
8. Navarro, J.F. and C. Mora, *Role of inflammation in diabetic complications.* Nephrology dialysis transplantation, 2005. **20**(12): p. 2601-2604.
9. Wei, H., et al., *Complications following stem cell therapy in inflammatory bowel disease.* Current stem cell research & therapy, 2017. **12**(6): p. 471-475.
10. Master, Z., M. McLeod, and I. Mendez, *Benefits, risks and ethical considerations in translation of stem cell research to clinical applications in Parkinson's disease.* Journal of Medical Ethics, 2007. **33**(3): p. 169-173.
11. Jarajapu, Y.P. and M.B. Grant, *The promise of cell-based therapies for diabetic complications: challenges and solutions.* Circulation research, 2010. **106**(5): p. 854-869.
12. Pollack, R.M., et al., *Anti-inflammatory agents in the treatment of diabetes and its vascular complications.* Diabetes Care, 2016. **39**(Supplement 2): p. S244-S252.
13. Rauter, I., et al., *Mast cell–derived proteases control allergic inflammation through cleavage of IgE.* Journal of Allergy and Clinical Immunology, 2008. **121**(1): p. 197-202.
14. Tang, F., et al., *Inhibitory effect of methyleugenol on IgE-mediated allergic inflammation in RBL-2H3 cells.* Mediators of inflammation, 2015. **2015**.
15. Nadler, M., et al., *Signal transduction by the high-affinity immunoglobulin E receptor FcRI: coupling form to function.* Adv. Immunol, 2000. **76**: p. 325-355.
16. Turner, H. and J.-P. Kinet, *Signalling through the high-affinity IgE receptor FcεRI.* Nature, 1999. **402**(6760supp): p. 24.

17. Bissell, M.J., A. Rizki, and I.S. Mian, *Tissue architecture: the ultimate regulator of breast epithelial function.* Current opinion in cell biology, 2003. **15**(6): p. 753.
18. Wozniak, M.A., et al., *ROCK-generated contractility regulates breast epithelial cell differentiation in response to the physical properties of a three-dimensional collagen matrix.* J Cell Biol, 2003. **163**(3): p. 583-595.
19. Stachowiak, A.N., et al., *Bioactive hydrogels with an ordered cellular structure combine interconnected macroporosity and robust mechanical properties.* Advanced Materials, 2005. **17**(4): p. 399-403.
20. Church, M.K. and F. Levi-Schaffer, *The human mast cell.* Journal of Allergy and Clinical Immunology, 1997. **99**(2): p. 155-160.
21. Costa, J.J., P.F. Weller, and S.J. Galli, *The cells of the allergic response: mast cells, basophils, and eosinophils.* Jama, 1997. **278**(22): p. 1815-1822.
22. Krishnaswamy, G., et al., *Regulation of eosinophil-active cytokine production from human cord blood-derived mast cells.* Journal of interferon & cytokine research, 2002. **22**(3): p. 379-388.
23. Marone, G., et al., *Molecular and cellular biology of mast cells and basophils.* International archives of allergy and immunology, 1997. **114**(3): p. 207-217.
24. Galli, S.J. and B.K. Wershil, *The two faces of the mast cell.* Nature, 1996. **381**(6577): p. 21.
25. Fung-Leung, W.-P., et al., *Transgenic mice expressing the human high-affinity immunoglobulin (Ig) E receptor alpha chain respond to human IgE in mast cell degranulation and in allergic reactions.* Journal of Experimental Medicine, 1996. **183**(1): p. 49-56.
26. Abraham, S.N., K. Thankavel, and R. Malaviya, *Mast cells as modulators of host defense in the lung.* Frontiers in bioscience: a journal and virtual library, 1997. **2**: p. d78-87.
27. Bischoff, S.C., *Role of mast cells in allergic and non-allergic immune responses: comparison of human and murine data.* Nature Reviews Immunology, 2007. **7**(2): p. 93.
28. Bradding, P., *Human mast cell cytokines.* Clinical & Experimental Allergy, 1996. **26**(1): p. 13-19.
29. Bradding, P. and S.T. Holgate, *The mast cell as a source of cytokines in asthma.* Annals of the New York Academy of Sciences, 1996. **796**(1): p. 272-281.
30. Krishnaswamy, G., et al., *Multifunctional cytokine expression by human mast cells: regulation by T cell membrane contact and glucocorticoids.* Journal of interferon & cytokine research, 1997. **17**(3): p. 167-176.
31. Plaut, M., et al., *Mast cell lines produce lymphokines in response to cross-linkage of FcεRI or to calcium ionophores.* Nature, 1989. **339**(6219): p. 64.
32. Mekori, Y.A. and D.D. Metcalfe, *Mast cell–T cell interactions.* Journal of Allergy and Clinical Immunology, 1999. **104**(3): p. 517-523.
33. Walsh, L.J., et al., *Human dermal mast cells contain and release tumor necrosis factor alpha, which induces endothelial leukocyte adhesion molecule 1.* Proceedings of the National Academy of Sciences, 1991. **88**(10): p. 4220-4224.
34. Malaviya, R., et al., *Mast cell modulation of neutrophil influx and bacterial clearance at sites of infection through TNF-α.* Nature, 1996. **381**(6577): p. 77.

35. Barsumian, E.L., et al., *Establishment of four mouse mastocytoma cell lines.* Cellular immunology, 1985. **90**(1): p. 131-141.
36. Pierce, J.H., et al., *Neoplastic transformation of mast cells by Abelson-MuLV: abrogation of IL-3 dependence by a nonautocrine mechanism.* Cell, 1985. **41**(3): p. 685-693.
37. Siraganian, R.P., *Mast cell signal transduction from the high-affinity IgE receptor.* Current opinion in immunology, 2003. **15**(6): p. 639-646.
38. Taurog, J.D., et al., *Noncytotoxic IgE-mediated release of histamine and serotonin from murine mastocytoma cells.* The Journal of Immunology, 1977. **119**(5): p. 1757-1761.
39. Denburg, J.A. *Cytokine-induced human basophil/mast cell growth and differentiation in vitro*. in *Springer seminars in immunopathology*. 1990. Springer.
40. Iemura, A., et al., *The c-kit ligand, stem cell factor, promotes mast cell survival by suppressing apoptosis.* The American journal of pathology, 1994. **144**(2): p. 321.
41. Ishizaka, T., et al., *development of mast cells in vitro: II. Biologic function of cultured mast cells.* The Journal of Immunology, 1977. **118**(1): p. 211-217.
42. Keller, G., et al., *Hematopoietic commitment during embryonic stem cell differentiation in culture.* Molecular and cellular biology, 1993. **13**(1): p. 473-486.
43. Nakano, T., et al., *Fate of bone marrow-derived cultured mast cells after intracutaneous, intraperitoneal, and intravenous transfer into genetically mast cell-deficient W/Wv mice. Evidence that cultured mast cells can give rise to both connective tissue type and mucosal mast cells.* Journal of Experimental Medicine, 1985. **162**(3): p. 1025-1043.
44. Valent, P., C. Sillaber, and P. Bettelheim, *The growth and differentiation of mast cells.* Progress in growth factor research, 1991. **3**(1): p. 27-41.
45. Andersen, H.B., et al., *Comparison of short term in vitro cultured human mast cells from different progenitors—peripheral blood-derived progenitors generate highly mature and functional mast cells.* Journal of immunological methods, 2008. **336**(2): p. 166-174.
46. Schmetzer, O., et al., *A novel method to generate and culture human mast cells: peripheral CD34+ stem cell-derived mast cells (PSCMCs).* Journal of immunological methods, 2014. **413**: p. 62-68.
47. Matsuzawa, S., et al., *IL-9 enhances the growth of human mast cell progenitors under stimulation with stem cell factor.* The Journal of Immunology, 2003. **170**(7): p. 3461-3467.
48. Valent, P., et al., *Induction of differentiation of human mast cells from bone marrow and peripheral blood mononuclear cells by recombinant human stem cell factor/kit-ligand in long-term culture.* Blood, 1992. **80**(9): p. 2237-2245.
49. Rådinger, M., et al., *Generation, isolation, and maintenance of human mast cells and mast cell lines derived from peripheral blood or cord blood.* Current protocols in immunology, 2010. **90**(1): p. 7.37. 1-7.37. 12.
50. Saito, H., *Culture of human mast cells from hemopoietic progenitors*, in *Mast Cells*. 2006, Springer. p. 113-122.
51. Kirshenbaum, A.S., et al., *Demonstration that human mast cells arise from a progenitor cell population that is CD34+, c-kit+, and expresses aminopeptidase N (CD13).* Blood, 1999. **94**(7): p. 2333-2342.

52. Derakhshan, T., et al., *Development of human mast cells from hematopoietic stem cells within a 3D collagen matrix: effect of stem cell media on mast cell generation.*
53. Liu, C., et al., *Molecular regulation of mast cell development and maturation.* Molecular biology reports, 2010. **37**(4): p. 1993-2001.
54. Mierke, C.T., et al., *Human endothelial cells regulate survival and proliferation of human mast cells.* Journal of Experimental Medicine, 2000. **192**(6): p. 801-812.
55. Livak, K.J. and T.D. Schmittgen, *Analysis of relative gene expression data using real-time quantitative PCR and the 2− ΔΔCT method.* methods, 2001. **25**(4): p. 402-408.
56. Thon, I. and B. Uvnäs, *Mode of storage of histamine in mast cells.* Acta Physiologica, 1966. **67**(3-4): p. 455-470.
57. Saito, H., et al., *Human mast cell colony-forming cells in culture.* International archives of allergy and immunology, 2001. **124**(1-3): p. 301-303.
58. Yamamoto, T., et al., *Mast cells enhance contraction of three-dimensional collagen lattices by fibroblasts by cell–cell interaction: role of stem cell factor/c-kit.* Immunology, 2000. **99**(3): p. 435-439.
59. de Souza Junior, D.A., et al., *Mast Cells Interact with Endothelial Cells to Accelerate In Vitro Angiogenesis.* International journal of molecular sciences, 2017. **18**(12): p. 2674.
60. Metcalfe, D.D., D. Baram, and Y.A. Mekori, *Mast cells.* Physiological reviews, 1997. **77**(4): p. 1033-1079.
61. Schulman, E., et al., *Heterogeneity of human mast cells.* The Journal of Immunology, 1983. **131**(4): p. 1936-1941.
62. Yong, L., *The mast cell: origin, morphology, distribution, and function.* Experimental and Toxicologic Pathology, 1997. **49**(6): p. 409-424.
63. Leclere, M., et al., *Comparison of four staining methods for detection of mast cells in equine bronchoalveolar lavage fluid.* Journal of veterinary internal medicine, 2006. **20**(2): p. 377-381.
64. Ribatti, D., *The Staining of Mast Cells: A Historical Overview.* International archives of allergy and immunology, 2018. **176**(1): p. 55-60.
65. Helander, H.F. and G.D. Bloom, *Quantitative analysis of mast cell structure.* Journal of microscopy, 1974. **100**(3): p. 315-321.
66. Theoharides, T.C., et al., *Mast cells and inflammation.* Biochimica et Biophysica Acta (BBA)-Molecular Basis of Disease, 2012. **1822**(1): p. 21-33.
67. Philpott, N., et al., *G-CSF-mobilized CD34+ peripheral blood stem cells are significantly less apoptotic than unstimulated peripheral blood CD34+ cells: role of G-CSF as survival factor.* British journal of haematology, 1997. **97**(1): p. 146-152.
68. Hartung, T., et al., *How to leverage an endogenous immune defense mechanism: the example of granulocyte colony-stimulating factor.* Critical care medicine, 2003. **31**(1): p. S65-S75.
69. Hui, N. and N. Le Marer, *α-2, 6-Sialylation regulation in CD34+ progenitor cells in the human bone marrow and granulocyte colony-stimulating factor mobilization.* Journal of hematotherapy & stem cell research, 2001. **10**(5): p. 661-668.

70. Yang, F.-C., et al., *Human granulocyte colony-stimulating factor (G-CSF) stimulates the in vitro and in vivo development but not commitment of primitive multipotential progenitors from transgenic mice expressing the human G-CSF receptor.* Blood, 1998. **92**(12): p. 4632-4640.
71. Toru, H., et al., *Induction of the high-affinity IgE receptor (FcεRI) on human mast cells by IL-4.* International immunology, 1996. **8**(9): p. 1367-1373.
72. Osterhoff, B., et al., *Immunomorphologic Characterization of Fc∈RI-Bearing Cells Within the Human Dermis.* Journal of investigative dermatology, 1994. **102**(3).
73. Amin, K., *The role of mast cells in allergic inflammation.* Respiratory medicine, 2012. **106**(1): p. 9-14.
74. Ulich, T., et al., *Hematologic effects of stem cell factor alone and in combination with G-CSF and GM-CSF in vivo and in vitro in rodents.* International review of experimental pathology, 1993. **34**: p. 215-233.
75. Williams, C.M. and S.J. Galli, *The diverse potential effector and immunoregulatory roles of mast cells in allergic disease.* Journal of Allergy and Clinical Immunology, 2000. **105**(5): p. 847-859.
76. Sayama, K., et al., *Transcriptional response of human mast cells stimulated via the FcεRI and identification of mast cells as a source of IL-11.* BMC immunology, 2002. **3**(1): p. 5.
77. Möller, A., et al., *Comparative cytokine gene expression: regulation and release by human mast cells.* Immunology, 1998. **93**(2): p. 289.
78. Caughey, G.H., *Mast cell proteases as protective and inflammatory mediators*, in *Mast Cell Biology*. 2011, Springer. p. 212-234.
79. Gao, Y., et al., *TNF-α Regulates Mast Cell Functions by Inhibiting Cell Degranulation.* Cellular Physiology and Biochemistry, 2017. **44**(2): p. 751-762.
80. Nakae, S., et al., *Mast cells enhance T cell activation: importance of mast cell costimulatory molecules and secreted TNF.* The Journal of Immunology, 2006. **176**(4): p. 2238-2248.
81. Dahl, C., et al., *Human mast cells express receptors for IL-3, IL-5 and GM-CSF; a partial map of receptors on human mast cells cultured in vitro.* Allergy, 2004. **59**(10): p. 1087-1096.
82. Kinoshita, M., et al., *Mast cell tryptase in mast cell granules enhances MCP-1 and interleukin-8 production in human endothelial cells.* Arteriosclerosis, thrombosis, and vascular biology, 2005. **25**(9): p. 1858-1863.

VITA

Tszwai Regina Chan

Candidate for the Degree of

Master of Science

Thesis: USING A TISSUE-ENGINEERED VASCULAR MODEL TO DEVELOP MAST CELLS FROM ADULT STEM CELLS

Major Field: Chemical Engineering

Education:

Completed the requirements for the Master of Science in chemical engineering at Oklahoma State University, Stillwater, Oklahoma in July, 2018.

Completed the requirements for the Bachelor of Science in chemical engineering at Arizona State University, Tempe, AZ in 2011.

Experience:

Worked as Graduate Research Assistant in the School of Chemical Engineering at Oklahoma State University, Stillwater from June 2016 to July 2018